EEG-fNIRS based hybrid Image reconstruction and classification for BCI

Author

Nabeeha Ehsan Mughal

Regn Number

00000276125

Supervisor

Dr. Muhammad Jawad Khan

DEPARTMENT OF ROBOTICS AND INTELLIGENT MACHINE ENGINEERING

SCHOOL OF MECHANICAL & MANUFACTURING ENGINEERING

NATIONAL UNIVERSITY OF SCIENCES AND TECHNOLOGY

ISLAMABAD

FEBURARY 2021

EEG-fNIRS based hybrid Image reconstruction and classification for BCI

Author

Nabeeha Ehsan Mughal

Regn Number

00000276125

A thesis submitted in partial fulfillment of the requirements for the degree of

MS Robotics and Intelligent Machine Engineering

Thesis Supervisor:

Dr. Muhammad Jawad Khan

Thesis Supervisor's Signature: _____

DEPARTMENT OF ROBOTICS AND INTELLIGENT MACHINE ENGINEERING

SCHOOL OF MECHANICAL & MANUFACTURING ENGINEERING

NATIONAL UNIVERSITY OF SCIENCES AND TECHNOLOGY, ISLAMABAD

FEBURARY 2021

Thesis Acceptance Certificate

It is certified that the final copy of MS Thesis written by **Nabeeha Ehsan Mughal** (Registration No. **00000276125**), of Department of **Robotics and Intelligent Machine Engineering (SMME)** has been vetted by undersigned, found complete in all respects as per NUST statutes / regulations, is free from plagiarism, errors and mistakes and is accepted as a partial fulfilment for award of MS Degree. It is further certified that necessary amendments as pointed out by GEC members of the scholar have also been incorporated in this dissertation.

Signature:_____

Date:_____
Dr. Muhammad Jawad Khan (Supervisor)

Signature HOD:_____

Date:_____

Signature Principal:_____

Date:_____

FORM TH-4

National University of Sciences & Technology

MASTER THESIS WORK

We hereby recommend that the dissertation prepared under our supervision by: (Student Name & Regn No.) **Nabeeha Ehsan Mughal, 276125** Titled: **EEG-Fnirs Based Hybrid Image Reconstruction and Classification For BCI** be accepted in partial fulfillment of the requirements for the award of **MS** degree.

Examination Committee Members

1. Name: Dr. Kashif Javed Signature:_____
2. Name: Dr. Omer Gillani Signature:_____
3. Name: Dr. Hasan Sajid Signature:_____

Supervisor's name: Signature:_____

Dr. Muhammad Jawad Khan Date:_____

_____ _____

Head of Department Date

COUNTERSINGED

Date:_____ _____

Dean/Principal

Declaration

I certify that this research work titled "*EEG-fNIRS based hybrid Image reconstruction and classification for BCI"* is my own work. The work has not been presented elsewhere for assessment. The material that has been used from other sources it has been properly acknowledged / referred.

Signature of Student

Nabeeha Ehsan Mughal

NUST-SMME-MS-RIME 276125

Plagiarism Certificate (Turnitin Report)

This thesis has been checked for Plagiarism. Turnitin report endorsed by Supervisor is attached.

Signature of Student

Nabeeha Ehsan Mughal

Registration Number

00000276125

Signature of Supervisor

Dr. Muhammad Jawad Khan

Copyright Statement

Acknowledgments

First and foremost, praises and thanks to the Allah, the Almighty, for His showers of blessings throughout my research work to complete the research successfully and guiding me throughout this work at every step and for setting up every new thought in my mind to improve it.

I would like to express my deep and sincere gratitude to my research supervisor, Dr. Muhammad Jawad Khan Assistant Professor, Robotics and Intelligent Machine Engineering Department, National University of Science and Technology, Pakistan, for giving me the opportunity to do research and providing invaluable guidance throughout this research. His dynamism, vision, sincerity and motivation have deeply inspired me. He has taught me the methodology to carry out the research and to present the research works as clearly as possible. It was a great privilege and honor to work and study under his guidance. I am extremely grateful for what he has offered me.

I would also like to thank Dr. Hasan Sajid, Dr. Omer Gillani, and Dr. Kashif Javed for guiding and evaluating my work and express my special thanks to Khurram Khalil for his help. I am also thankful to Maira Ehsan for her support and cooperation.

I am profusely thankful to my beloved parents for supporting me in every department of my life. Finally, I would like to express my gratitude to all the individuals who have rendered valuable assistance to my study.

Dedicated to family and friends for their endless support and love.

Abstract

The ever-increasing human-machine interaction and advancement in socio-technical systems have made it essential to analyze the vital human factors such as mental workload, vigilance, fatigue, and stress, etc via monitoring brain states. Similarly, brain signals are becoming paramount for rehabilitation and assistive purposes in fields such as brain-computer interface (BCI), closed-loop neuromodulation for neurological disorders, etc. The complex, non-stationary, and very low signal-to-noise ratio of brain signals poses a significant challenge for researchers to design robust and reliable BCI systems outside the laboratory environment. In this work, I have presented a novel recurrence plots (RPs) based time-distributed convolutional neural network and long short term memory (CNN-LSTM) algorithm for four class functional near-infrared spectroscopy (fNIRS) BCI, electroencphelography (EEG) BCI and Hybrid EEG-fNIRS BCI. The acquired brain signals are projected into a non-linear dimension with RPs and fed into the CNN which extracts the important features and then LSTM learns the chronological and time-dependent relations. The average accuracy achieved with the proposed model is 79.7% with fNIRS 83.6% with EEG and 88.5%. for hybrid EEG-Fnirs BCI. While the maximum accuracies achieved are 85.9%, 88.1% and 92.4%, respectively. The results confirm the viability of RPs based deep learning algorithm for successful BCI systems.

Key Words: *BCI, fNIRS, EEG, Recurrence Plots (RP), Convolutionl Neural Networks (CNN), Long-Short Term Memory (LSTM), Time distributional layers*

Table of Contents

List of Figures

List of Tables

CHAPTER 1: INTRODUCTION

The research work in this dissertation has been presented in multiple parts. The first part is related to the detailed literature review of electroencephalography (EEG) and functional near-infrared spectroscopy (fNIRS) based brain-computer interface (BCI), hybrid EEG-fNIRS based BCI, different machine learning (ML) and deep learning (DL) algorithms used for classification for BCI and use of recurrence analysis in BCI. The next part includes the detailed methodology adopted for classification of 4-class EEG-BCI, fNIRS-BCI and hybrid EEG-fNIRS-BCI using recurrence plots. Further in the line, the detailed results for all three cases of BCI are presented. Lastly, the results are discussed and concluded in the last section.

1.1 Background

1.1.1 Brain Computer Interface

Brain Computer Interface (BCI) is becoming an indispensable element for individuals who are unable to control their muscular activities due to neuromuscular disorder, stroke, Locked-in syndrome (LIS), spinal injuries, or amyotrophic lateral sclerosis (ALS) [1]. BCI has become the integral component of the contemporary medical application, but the applications of the BCI cannot be limit just here, the BCI has strengthened its roots in the communication systems, human-machine interfaces (HMI), and neurofeedback applications [2],[3]. The BCI communicates between the human brain and the external computer/device through generated brain commands avoiding the peripheral nervous system [4]. BCI is among such neurofeedback methods that can enhance the condition of life of patients suffering from serious motor debilities due to tetraplegia, stroke, ad other spinal cord injuries [5]. BCI has also applications in neuro-rehabilitation, communication and control, motor therapy and recovery, brain monitoring, and neuro-ergonomics [6],[7],[8].

BCI works by taking a bio-signal measured from a healthy/patient subject and based on that predicts some intangible aspects of his/her cognitive state. Usually a BCI systems has three main steps involved: first is data acquisition from brain depending on the application and modality chosen, next is to interpret or processes acquired data to commands, and last step is outputting commands to a connected computer/ machine to execute any action. Among the three types of BCI i.e., reactive, active, and passive BCI, passive BCI (pBCI) is an important research area in BCI

that is mainly focused on the estimation of human emotions, cognition, intentions and behavior from generated brain responses to different situations. With the advancement in neuroimaging modalities, the demand for improvement in traditional BCI practices is also increasing. The major non-invasive BCI modalities include fMRI, EEG, MEG, and fNIRS. Among these non-invasive BCI modalities, EEG, and fNIRS are the foremost modalities in terms of price and manageability [9],[10]. EEG measures brain activity by calculating the voltage fluctuations from neurons' action potentials while fNIRS detects the brain activity concerning the changes in hemodynamic response [11],[12].

1.1.2 Hybrid EEG-fNIRS BCI

Though the invasive techniques provide considerably accurate data than the non-invasive techniques. But the use of non-invasive modalities is more frequent and appreciated in the research domain. For recording the brain activities non-invasive techniques not only provide safety but also exempts ethical concerns [13],[14]. Over time various non-invasive techniques have found their way into the research the most commonly used are electroencephalography (EEG), functional near-infrared spectroscopy (fNIRS), electrooculography (EOG), and functional magnetic resonance imaging (fMRI) [15],[16]. Each modality has offered some pros over the other, there are always some tradeoffs associated with the selection of the non-invasive modality according to the application. The choice is made for the modality depending upon many factors, usually, the following parameters are put into consideration, the cost, the ease of use, temporal and spatial resolution as needed by the application. As described earlier there are tradeoffs associated with each modality, the pros of one modality compensate the cons of the other modality thus the hybrid approaches are proving to be more efficient. The hybrid neuroimaging modalities not only increase the accuracy but also offer a greater degree of credible control [17-19].

Researchers highly appreciate the low-cost neuroimaging modalities. The modalities which offer the non-laboratory setup convenience usually are the choice of interest too. The most commonly used neuroimaging modalities in this respect are EEG and fNIRS. Both the modalities are portable as well as low cost as compared to the others. EEG signal is captured by the electrodes as a result of current variation in the neurons due to postsynaptic activities [20]. For the EEG data acquisition, several electrodes are placed on the scalp of the subject. EEG provides better temporal resolution. The resolution ranges up to 0.05 seconds approximately. However, EEG does not have

a good spatial resolution. The spatial resolution is approximately around 10mm [21],[22]. The contrasting comparison of the temporal and spatial resolution manifests the tradeoffs while using the EEG modality. In contrast to the EEG, fNIRS constructs the functional neuroimages of the brain by employing near-infrared light. The NIR light measures the blood oxygen level dependence (BOLD). Like EEG fNIRS is low cost and portable too. But unlike EEG, fNIRS provide a better spatial resolution. Moreover, fNIRS is also less influence by electrical noises [23]. As evident by the comparison that the tradeoffs of the EEG modality can be compensated by fNIRS. Thus, on the theoretical grounds, the hybrid of the EEG and fNIRS should prove itself as a breakthrough in neuroimaging [24].

Since fNIRS measures the hemodynamic responses, so it is bind with an innate delay in the measurement [25]. Various methods have been offered in this regard to compensate for this conducive slow command generation. EEG and fNIRS hybrid can to compensate for the delayed response of the fNIRS modality. Moreover, the measurement of the initial dip (i.e., at the onset of the neural firing the HBO level first falls) instead of the actual hemodynamic response [26],[27]. The other contrasting difference between both the modalities is the rate at which data is sampled. The EEG data acquisition rate is approximately 10-100 times swifter than the fNIRS. When the EEG and fNIRS hybrid is intended to use then it is a common practice to down sample the EEG data to make its processing compatible with the fNIRS data [28],[29]. The down sampling might discard some chunks of the valuable data. As EEG signal is prone to electrical noises similarly the fNIRS suffer from physiological noises, instrumentation, and experimental errors. The experimental errors can be the spontaneous unintentional diversion from the intended protocol like the motion artifacts or the changing light intensity in the ambiance. The motion artifacts present in the data can be significantly reduced via wiener filtering-based methods [30] or wavelet analysis-based methods [31]. The instrumentation can also induce noise in the data, like the noises from the hardware, though these noises are high-frequency components thus can be eliminated by using a low-pass filter. The physiological noises can arise as a result of breathing activity or from the heartbeat, these noises are unavoidable, yet the literature has shown many methods to counter these noises, the commonly used techniques are using bandpass filters; parameter mapping, and individual component analysis [32-34]. Denoising the data further remove the chunks of data; thus the processed data is even smaller in magnitude than raw. The down sampling of the EEG data to

match the fNIRS data after preprocessing removes a considerable amount of valuable information regarding brain activity. Literature review of hybrid EEG-fNIRS BCI is given in below table.

Table 1-1: Literature review of Hybrid EEG-fNIRS BCI

	Year	Modality	Objective	Brain Area	Methodology	Results
1	**Visual evoked nerve cerebral oxygen characteristics analysis based on NIRS-EEG**					
	2018	Hybrid NIRS-EEG	Relation between electrophysiological And hemodynamic responses to a checkerboard stimulus reversing.	Visual cortex	Linear regression analysis	Linear relationship
2	**A hybrid NIRS-EEG system for self-paced brain-computer interface with online motor imagery**					
	2014	Hybrid NIRS-EEG	Analysis method that detects the occurrence of motor imagery with the NIRS system and classifies its type with the EEG system.	Primary motor cortex	Thresholding to detect motor imagery from NIRS signal. Linear-SVM classifier for classification of left- or right-hand motor imagery.	True positive rate of about 88%, a false positive rate of 7% with an average response time of 10.36 s.
3	**NIRS-EEG joint imaging during transcranial direct current stimulation: Online parameter estimation with an autoregressive model**					
	2016	Hybrid NIRS-EEG	Online resting-state spontaneous brain activation may be relevant to monitor tDCS neuromodulatory effects that can be measured using electroencephalography (EEG) in conjunction with near-infrared spectroscopy (NIRS).	Left primary sensorimotor cortex	Kalman Filter based online parameter estimation of an autoregressive (ARX) model.	Kalman Filter based method allowed online ARX parameter estimation using time-varying signals that could capture transients in the coupling relationship between EEG and NIRS signals.

4	**A Mobile, Modular, Multimodal Bio-signal Acquisition Architecture for Miniaturized EEG-NIRS-Based Hybrid BCI and Monitoring**					
	2017	Hybrid NIRS-EEG	Objective was to design such an instrument in a miniaturized, customizable, and wireless form.	Left fronto-parietal region	The design and evaluation of a mobile, modular, multimodal bio-signal acquisition architecture (M3BA) based on a high-performance analog front-end optimized for biopotential acquisition, a microcontroller, and open- NIRS technology is presented.	The designed M3BA modules are very small configurable high-precision and low-noise modules. They support flexible user-specified biopotential reference setups and wireless body area/sensor network scenarios.
5	**Imagined Hand Clenching Force and Speed Modulate Brain Activity and Are Classified by NIRS Combined With EEG**					
	2017	Hybrid NIRS-EEG	6-class classification of the imagined motor parameters by NIRS-EEG.	Sensorimotor area	SVM classifier	1) HbO-HbD (60-69%) 2) IA-IP-IF (70-74%) 3) Combined (71-78%)
6	**Hybrid EEG-NIRS based active command generation for quadcopter movement control**					
	2016	Hybrid NIRS-EEG	Four active commands for quadcopter control in online environment.	Prefrontal cortex	Linear discriminant analysis (LDA)	1) Mental arithmetic (avg. 86.6%) 2) Left-clenching Imagery (avg. 78.1) 3) Eye- movement (avg. 86.9) 4) SSVEP (avg. 87.2)
7	**Long-term Monitoring of NIRS and EEG Signals for Assessment of Daily Changes in Emotional Valence**					
	2018	Hybrid NIRS-EEG	The indices of frontal alpha asymmetry (FAA) obtained from electroencephalography (EEG) data in the resting state, laterality index at rest (LIR) from near infrared spectroscopy (NIRS) data and CVM are compared with BDI and STAI scores.	Frontal and Prefrontal cortex	Correlations analysis	The correlations require further analysis with sample data obtained over longer periods so that a regression model can be developed. These experimental results suggest that FAA, LIR, and emotional valence of CVM can be diagnostic markers for assessment of daily changes in emotional valence.
8	**EEG-NIRS Based Assessment of Neurovascular Coupling During Anodal Transcranial Direct Current Stimulation - a Stroke Case Series**					
	2015	Hybrid NIRS-EEG	A method for the assessment of NVC underlying the site of anodal tDCS.	Anode at C_z and cathode over left supraorbital notch	Hilbert-Huang transform-based assessment of neurovascular coupling.	It was postulated that tDCS leads to rapid dynamic variations of the brain cell microenvironment that perturbs hemodynamic and electrophysiological responses.
9	**Utilization of a combined EEG/NIRS system to predict driver drowsiness**					
	2017	Hybrid NIRS-EEG	An approach is introduced, a combination of EEG and NIRS, to detect driver drowsiness.	All over brain	Fisher's linear discriminant analysis method	The mean accuracy of the combined EEG/NIRS increases 8.7 percent compared to EEG alone and 5.5 percent compared to NIRS alone.
10	**Open Access Dataset for EEG+NIRS Single-Trial Classification**					
	2017	Hybrid NIRS-EEG	An open access dataset is provided in this study for hybrid brain–computer interfaces (BCIs) using electroencephalography (EEG) and near-infrared spectroscopy (NIRS).		Baseline signal analysis methods	MI- and MA-related activations were classifiable over motor areas and front-parietal areas, respectively but the approach used led to rather poorer decoding accuracies.

11	**Open Access Repository for Hybrid EEG-NIRS Data**					
		Hybrid NIRS-EEG	The datasets contain BCI data such as motor imagery (MI)-, and mental arithmetic (MA), and word generation (WG)-related brain signals, and cognitive task data such as n-back (NB)-, and discrimination/selection response (DSR)-related brain signals.		1) Down sampling EEG data. 2) Band-pass filter. 3) ICA- for EOG rejection. 4) Common spatial patterns. 5) Linear discriminant analysis.	75.9 % and 86.2 % of the participants show improved performance by the hybrid approach for MI and MA, respectively. The performance of 74.2 % of the participants are significantly improved by the hybrid approach than EE.
12	**An EEG-NIRS Multimodal SoC for Accurate Anesthesia Depth Monitoring**					
	2018	Hybrid NIRS-EEG	A multimodal head-patch system that simultaneously measures EEG and near Infrared spectroscopy (NIRS) is proposed for monitoring accurate anesthesia depth.	Frontal lobe	Logarithmic transimpedance amplifier (TIA) and closed loop controlled (CLC) NIRS current driver	System is able to perform ketamine monitoring and electrical interference compensation as compared to BIS system.
13	**A Comparison of EEG and NIRS Biomarkers for Assessment of Depression Risk**					
	2018	Hybrid NIRS-EEG	This study assesses the Frontal Alpha Asymmetry (FAA) and Laterality Index at Rest (LIR) for detection of depression risk in the early stage.		Pearson's correlation analysis	These correlations need further analysis with sample data of longer periods so that a regression model to combine the potential biomarkers can be developed.
14	**Computational Pipeline for NIRS-EEG Joint Imaging of tDCS-Evoked Cerebral Responses—An Application in Ischemic Stroke**					
	2016	Hybrid NIRS-EEG	A software to target vascular territories with tDCS and develop a NIRS-EEG probe for joint imaging of tDCS-evoked responses.		Based on their prior work, a cross-correlation analysis approach is presented to capture the coupling relation between regional cerebral hemoglobin oxygen saturation and the log-transformed mean-power time-series for EEG in case of ischemic stroke survivor.	
15	**Multichannel Wearable fNIRS-EEG System for Long-Term Clinical Monitoring**					
	2018	Hybrid NIRS-EEG	A novel fNIRS-EEG stretchable cap, two analog channels for auxiliary data (e.g., electrocardiogram), eight digital triggers for event-related protocols and an internal accelerometer for movement artifacts removal contribute to improve data acquisition quality.		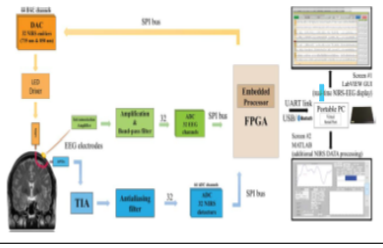	
16	**Study on Multi-parameter Evaluation Method of VDT Visual Fatigue Based on EEG and NIRS**					
	2017	Hybrid NIRS-EEG	A comprehensive and objective assessment of visual fatigue.		1. attend-to-ignore ratios (AIR) of SSVEP amplitude before and after experiment. 2. analyzed EEG data with eight octave wavelet decomposition. 3. Calculated energy of each frequency band. 4. Analyzed blood oxygen saturation levels.	The cerebral blood oxygen saturation would decrease because of visual fatigue. Results are almost consistent with previous relevant research.

1.1.3 Classification Approaches Used in BCI

The brain signals as captured by the EEG and fNIRS modalities is a time series data. The time-series data has many practical applications, that range from the regime of cybersecurity to bio signal processing. However, apart from their wide usage, the classification of the time series data poses issues. Machine learning algorithms have been developed to classify this time series-based data [35],[36]. One of the widely used classification technique is to extract temporal features from the data and feeding them as input to the classifier [37],[38]. Traditionally the classification of this time series data was based on the following parameters, i.e., instance and the features-based methods [39]. The instance-based classification technique focuses on measuring the resemblances between the training and test data. One of the popular examples of the instance-based classification are the KNN and dynamic time wrapping [40],[41]. While on the contrary the feature-based method applies a newer approach and transforms the data into a newer space. Unlike the instance-based classification method, this method focuses on the differences and discrimination of the test data [42]. This method has proven to be more efficient as compared to the instance based.

For the brain-computer interface applications, the CNN can be employed in two ways, the first being is the alteration or modification of the CNN algorithm architecture to accommodate the 1-dimensional time-series data obtained by the modalities. Or 1-dimensional data can be transformed into the 2dimensional data and then can be conveniently put as an input to the CNN.DNN along with the other traditional classifiers have also been employed on the fNIRS signals to recognize three different cognitive states [43],[44]. A similar approach has been used for various other applications, i.e., controlling the robots [45-48], differentiated the different levels of the workloads by analyzing the fNIRS signal and using deep learning techniques. Literature also manifests the use of the time-delay neural network (TDNN) for classification purposes. [49] used this approach to classify the EEG signal however the presented model was not deep enough to be capable of learning the hierarchical features of the EEG signal. The research that greatly resonated with our study under observation is [50], the author investigated deep learning based BCI for detection of driver drowsiness. The output strength of the selected channels was translated into the colormaps, the colormaps were then fed into the CNN classifier as an input. The output color maps were obtained as a result of the linear mapping of the values from the channel into the color intensity. Literature review on Classification approaches used in BCI is presented in table below.

Table 1-2: Literature review on Classification approaches used in BCI

Reference	**Classifier**	**Modality**
[26]	Bagged importance weighted LDA	EEG
[28]	Marginalized stacked denoising autoencoder	EEG
[32]	Selective instance transfer with active learning	EEG
[33]	C3, C4	EEG
[34]	Common Spatial Patterns (CSP) and LDA	EEG
[24]	Stationary subspace CSP (ssCSP)	EEG
[38]	Principal component analysis (PCA) based CSP	EEG
[43]	Extreme learning machine (ELM)	EEG
[44]	Domain adaptation SVM (DASVM)	EEG

1.1.4 Recurrence Analysis of Brain Signals

The brain signal captured through the modalities of the EEG and fNIRS exhibit the data in the format of 1-Dimensional time series data. The contemporary techniques of bio signal analysis have a higher inclination towards non-linear dynamics. One of the widely used technique is the

recurrence plot. The analysis hunts for the repeatability of the time series states and presents the output in the form of geometric structures. the characteristic features of the dynamics are estimated by analyzing the topology of these structures [51],[52].

Recurrence quantification analysis (RQA) of RP has become popular in recent years in analyzing brain activity because brain signals are both recurrent and dynamic in nature. RP in general terms is a non-linear evaluation method for recurrent and dynamic signals. It is a visualization displaying the recurrence occurances of states x(n) of a time signal in phase space. RQA is the analysis technique to quantify features of constructed RP. In literature, RQA features analysis has been used in EEG signal detection of epilepsy and Alzheimer's, coupling and synchronization in EEG of epileptic discharge etc. At different sleep stages the cortical function has also been analyzed using RP features. RQA analysis shows that unique RPs are extracted for different sleep stages [53]. Few studies have also used artificial neural network (ANN) and support-vector machines (SVM) to classify extracted RQA features. One study has used four-layer ANN for different EEG channels to predict the onset of seizures using RQA measures [54].

Deep neural networks (DNNs) on the other hand are highly efficient training classifiers resulting in better classification accuracies as compared to other ML classifiers, but only a few studies on application of these algorithms are available so far of their application in BCI [55], [56]. Only one study has used a CNN for binary classification of epileptic seizures from EEG using RP as images [57]. Effective application of biological feedback in BCI requires efficient and precise methods for motor activity detection and classification.

As machine learning has swiftly become a state-of-the-art analysis tool, so researchers are more considerate about finding the features for classification. The qualitative aspect of these recurrence plots can be used for classification. Various approaches have been used in this regard like in [58] the author exhibited the use of the video compression algorithms along with the distance measure of cross-reference plot. [59] employed the recurrence feature classification to measure the heart rate variability using the support vector machine, in [60] the recurrence feature classification technique was employed along with the support vector machine. Another common trend observed in the literature is the classification and visualization of these plots using deep learning techniques. The approach has been employed in [61] to recognize the intention of the user, i.e., determine g the behavior of the user. In [62] and [63] Convolutional neural networks

were used to recognize the convolutional neural network. Literature review of application of RP in brain signal analysis is given in below table.

Table 1-3: Literature review on recurrence analysis of brain signals

	Year	Modality	Objective	Methodology	Results
1	**Concealed face recognition analysis based on Recurrence Plots**				
	2011	EEG	Use of Recurrence Plots (RPs) in order to discriminate between guilty and innocent subjects, using their single-trial ERPs	EEG data recording during Guilty Knowledge Test (GKT) followed by recurrence plots and RQA parameters	Some RQA variables in guilty subjects are significantly higher than innocent ones. The results also showed that appearance of the P300 component can increase determinism and synchronization, in brains' signals
2	**Understanding Coupling and Synchronization in EEG of Epileptic Discharge Using Recurrence Plots with Varying Threshold**				
	2012	EEG	Understanding the synchronicity of epileptic discharge using the property of recurrence of dynamical systems	Evaluation of the synchronization index from the recurrence distribution of phase space with variations in the recurrence dynamics by varying the threshold	he results of synchronization index indicate that the enhanced synchronicity is observed during seizure and decreases to near baseline level following seizure
3	**EEG-based emotion recognition using Recurrence Plot analysis and K nearest neighbor classifier**				
	2013	EEG	The classification of EEG correlates on emotion using Recurrence Plot	Recurrence Plot analysis to extract thirteen non-linear features from EEG. Then compared with feature extraction method based on spectral power analysis. The K nearest neighbor is applied to classify extracted features into the emotional states	Performance rates of 58.05%, 64.56% and 67.42% for 3 classes of valence, arousal and liking

4	**Adaptive filtering of EEG and epilepsy detection using Recurrence Quantification Analysis**				
	2014	EEG	Adaptive filtering of Electroencephalogram (EEG) signal and epileptic seizure detection using Recurrence Quantification Analysis (RQA)	Adaptive filtering of EEG signal followed by its recurrence plot formation and recurrence quantification analysis to detect epilepsy	sensitivity and specificity, 97.4% and 93.5% respectively
5	**Detecting epileptic electroencephalogram by Recurrence Quantification Analysis**				
	2016	EEG	Quantitative analysis of epileptic patient's and healthy subject's EEG to detect epilepsy	Average Diagonal Length, a parameter from Recurrence Quantification Analysis (RQA), was calculated to analyze the difference between normal EEG and epileptic EEG in, quantitatively	Compared with the healthy control subjects, the epileptic EEG is more regular and more certain, meanwhile, it is Average Diagonal Length is longer
6	**Recurrence plot structure of motor-related human EEG**				
	2019	EEG	RP structure of EEG segments recorded in somatosensory cortex are related with motor executions	RP reconstruction of EMG and EEG data recorded during motor task accomplishment	In averaged EEG signal background activity is mostly characterized by the diagonal lines, while motor task execution is associated with increase of recurrence points density and the emergence of vertical and horizontal lines
7	**Time-frequency and recurrence quantification analysis detect limb movement execution from EEG data**				
	2019	EEG	Application of recurrence quantification analysis (RQA) in detection of motor-related electroencephalograms (EEG)	RQA to reveal transitions of mu-rhythm dynamics extracted from multichannel EEG recorded in motor cortex	The results show that the considering RQA measures of EEG in time-frequency domain one can effectively reveal dynamical features of motor-related brain activity
8	**Characterization of EEG Resting-state Activity in Alzheimer's Disease by Means of Recurrence Plot Analyses**				
	2019	EEG	Characterize EEG resting-state activity in Alzheimer's disease (AD) patient's vs healthy subjects based on recurrence quantification analysis	TREND, a linear regression coefficient over the recurrence point density RRτ and provides information on the non-stationarity of a process	These results suggest that the dynamic properties of EEG resting-state activity differ between controls and AD patients
9	**Classification of Epileptic Seizures using Recurrence Plots and Machine Learning Techniques**				
	2019	EEG	To explore reliable and faster binary classification algorithms to develop real time seizure detection system	EEG feature extraction based on the Recurrence Plots (RP), and Recurrence Quantification Analysis (RQA) and then their classification using Artificial Neural Network (ANN), Probabilistic Neural Network (PNN) and Support Vector Machine (SVM)	91.2 % highest binary class accuracy achieved with SVM
10	**Two Approaches to Machine Learning Classification of Time Series Based on Recurrence Plots**				
	2020	EEG	Binary classification of epileptic seizure from EEG using two ML classification approaches for quantitative analysis and image classification	Perceptron (with 7 layers) for quantitative analysis of Recurrence plots CNN (with 131 layer) for image (Recurrence plot) classification	97% with perceptron 98% with CNN

1.1.5 Challenges to Real-Time BCI

To use BCI out of the laboratory on daily basis, BCI needs to address several challenges such as robust signal acquisition, extracting valuable knowledge from the acquired raw brain signals (either electrical or hemodynamic) for control-command generation, etc [25][26]. Another main problem is the requirement of recalibrating the BCI system. The recalibration requirement is required for every new session and subject. Usually, the calibration time for electroencephalography (EEG) and functional Near-Infrared spectroscopy (fNIRS) based BCI systems may take up to 20 minutes to 30 minutes, depending upon the situations, for each new session [27][28]. This is a strenuous and exhausting in terms of total time that the subject healthy/ patient has to commence before the BCI system is completely practical again. Also, another reason for having a such lengthy adjustment time for neuroimaging-based BCI is due to the high dimensionality of EEG and fNIRS signals that have low signal-to-noise ratio (SNR) [29]. In order to successfully classify the correct brain states, obtained neuroimaging signals are usually implemented in four stages: first preprocessing, second feature extraction, third classification, and lastly command generation [30][31]. The extracted features from brain signals are used to train the classifier. The collection of neuroimaging data is very complicated and also expensive both in terms of time and cost that makes it very hard to develop a substantial-scale, high-quality marked dataset for the training of deep learning models. That results in limited trials available for training. From low SNR signals, it is extremely difficult to approximate probability distributions of the features, usually in the case of machine learning algos, using only a few trials of multi-dimensional brain signals. Another important factor is the non-stationary nature of fNIRS and EEG signals. The exact brain state depends on factors such as the psychological and mental states, concentration level, drowsiness, fatigue, anatomical differences between subjects, and statistical variations in the data [32][33]. The instrumental noise and experimental error such as fluctuation in electrodes impedance due to perspiring may also temper the acquired brain signals [34]. All these facts combine results in the trained classifier performing poorly on new session data. The different studies tried to address these challenges by exploiting different methods and algorithms while trying to keep the models' accuracy in an acceptable range [28][35-37].

The most important objective of all studies carried on BCI is to enhance real-time classification accuracies and reduce computational costs, with multiple commands, emphasizing the need to develop appropriate identification and classification methods for real-time BCI [7].

Usually, multichannel brain signal acquisition modality i.e., EEG, is used to analyze brain motor activity by different existing methods like time and frequency feature analysis, event-related synchronization- desynchronization analysis, common spatial or temporal patterns, and spatial-spectral decomposition. The back draw of many of these methods is they require high computational costs, thus less feasible to use for real-time BCI [8].

These conventional quantification and feature selection methods along with the use of simple machine learning (ML) classifiers have few challenges while implementing for real-time BCI. The conventional feature engineering methods involve multiple steps like feature extraction, feature selection, finding suitable combinations for multiple feature, and sometimes dimensionality drop from a comparatively small quantity of data, that often leads to multiple other problems like overfitting and biasness [5], [9]. These inherent constraints make it difficult for researchers to make adjustments around the constraints and therefore a lot of time is consumed in initial steps of analysis i.e. data mining and data preprocessing.

1.2 Motivation

Researchers highly appreciate the low-cost neuroimaging modalities. The modalities which offer the non-laboratory setup convenience usually are the choice of interest too. The most commonly used neuroimaging modalities in this respect are EEG and fNIRS. Both the modalities are portable as well as low cost as compared to the others. EEG signal is captured by the electrodes as a result of current variation in the neurons due to postsynaptic activities [64]. For the EEG data acquisition, several electrodes are placed on the scalp of the subject. EEG provides better temporal resolution. The resolution ranges up to 0.05 seconds approximately. However, EEG does not have a good spatial resolution. The spatial resolution is approximately around 10mm [65-66]. The contrasting comparison of the temporal and spatial resolution manifests the tradeoffs while using the EEG modality. In contrast to the EEG, fNIRS constructs the functional neuroimages of the brain by employing near-infrared light. The NIR light measures the blood oxygen level dependence (BOLD). Like EEG fNIRS is low cost and portable too. But unlike EEG, fNIRS provide a better spatial resolution. Moreover, fNIRS is also less influence by electrical noises [67]. As evident by the comparison that the tradeoffs of the EEG modality can be compensated by fNIRS. Thus, on the theoretical grounds, the hybrid of the EEG and fNIRS should prove itself as a breakthrough in neuroimaging [68].

Since fNIRS measures the hemodynamic responses, so it is bind with an innate delay in the measurement [69]. Various methods have been offered in this regard to compensate for this conducive slow command generation. EEG and fNIRS hybrid can too compensate for the delayed response of the fNIRS modality. Moreover, the measurement of the initial dip (i.e., at the onset of the neural firing the HBO level first falls) instead of the actual hemodynamic response [70],[71]. The other contrasting difference between both the modalities is the rate at which data is sampled. The EEG data acquisition rate is approximately 10-100 times swifter than the fNIRS. When the EEG and fNIRS hybrid is intended to use then it is a common practice to down sample the EEG data to make its processing compatible with the fNIRS data [72],[73]. The down sampling might discard some chunks of the valuable data. As EEG signal is prone to electrical noises similarly the fNIRS suffer from physiological noises, instrumentation, and experimental errors. The experimental errors can be the spontaneous unintentional diversion from the intended protocol like the motion artifacts or the changing light intensity in the ambiance. The motion artifacts present in the data can be significantly reduced via wiener filtering-based methods [74] or wavelet analysis-based methods [75]. The instrumentation can also induce noise in the data, like the noises from the hardware, though these noises are high-frequency components thus can be eliminated by using a low-pass filter. The physiological noises can arise as a result of breathing activity or from the heartbeat, these noises are unavoidable, yet the literature has shown many methods to counter these noises, the commonly used techniques are using bandpass filters; parameter mapping, and individual component analysis [76-78]. Denoising the data further remove the chunks of data; thus, the processed data is even smaller in magnitude than raw. The down sampling of the EEG data to match the fNIRS data after preprocessing removes a considerable amount of valuable information regarding brain activity.

The most important objective of all studies carried on BCI is to enhance real-time classification accuracies and reduce computational costs, with multiple commands, emphasizing the need to develop appropriate identification and classification methods for real-time BCI [79]. Usually, multichannel brain signal acquisition modality i.e., EEG, is used to analyze brain motor activity by different existing methods like time and frequency feature analysis, event-related synchronization- desynchronization analysis, common spatial or temporal patterns, and spatial-spectral decomposition. The back draw of many of these methods is they require high computational costs, thus less feasible to use for real-time BCI [80].

These conventional quantification and feature selection methods along with the use of simple machine learning (ML) classifiers have few challenges while implementing for real-time BCI. The conventional feature engineering methods involve multiple steps like feature extraction, feature selection, finding suitable combinations for multiple feature, and sometimes dimensionality drop from a comparatively small quantity of data, that often leads to multiple other problems like overfitting and biasness [5], [9]. These inherent constraints make it difficult for researchers to make adjustments around the constraints and therefore a lot of time is consumed in initial steps of analysis i.e. data mining and data preprocessing.

1.3 Novelty

In this study, I have investigated the performance of Recurrence Plots (RP) for EEG, fNIRS and Hybrid EEG-fNIRS within the deep CNN-LSTM model for neuroimaging brain data for BCI. RP transforms the time series data into the image space and provides an alternate way to envisage the periodic nature of trajectory of a time series in phase space. RP helps us in exploring specific features of the multi-dimensional phase space trajectory using a 2D visualization. In last few years RP have been used for recurrence analysis of EEG for different applications but either using RQA or with ML classifiers using extracted features from RQA. In my work I have used RP of EEG and fNIRS as images to feed into the hybrid CNN-LSTM network for classification. Furthermore, I have implemented time-distributional layers in my network that are not being used in field of BCI before.

1.4 Structure of Research

The rest of the manuscript is devised as follows: Chapter 2 explains the detailed methodology of this research, the dataset used, RP formation from EEG and fNIRS dataset and the classification approach used for 4-class classification of constructed RP, in Chapters 3 the results are discussed related performance of RP in EEG-BCI, fNIRS-BCI and hybrid EEG-fNIRS-BCI. Chapter 4 compares the results from three BCI protocols with previous studies and conclude.

CHAPTER 2: RECURRENCE PLOTS AND CLASSIFICATION METHODOLOGY

In this study, the performance of Recurrence Plots (RP) for EEG, fNIRS and Hybrid EEG-fNIRS within the deep CNN-LSTM model is investigated for neuroimaging brain data for BCI. RP transforms the time series data into the image space and provides an alternate way to envisage the periodic nature of a trajectory of a time series in phase space. RP helps us in exploring specific features of the multi-dimensional phase space trajectory using a 2D visualization. In last few years RP have been used for recurrence analysis of EEG for different applications but either using RQA or with ML classifiers using extracted features from RQA. In this work RPs of EEG and fNIRS are used as images to feed into the hybrid CNN-LSTM network for classification. Furthermore, I have implemented time-distributional layers in my network that are not being used in field of BCI before. Detailed methodology is covered in this section. The methodology adopted for the study is shown in figure 2-1.

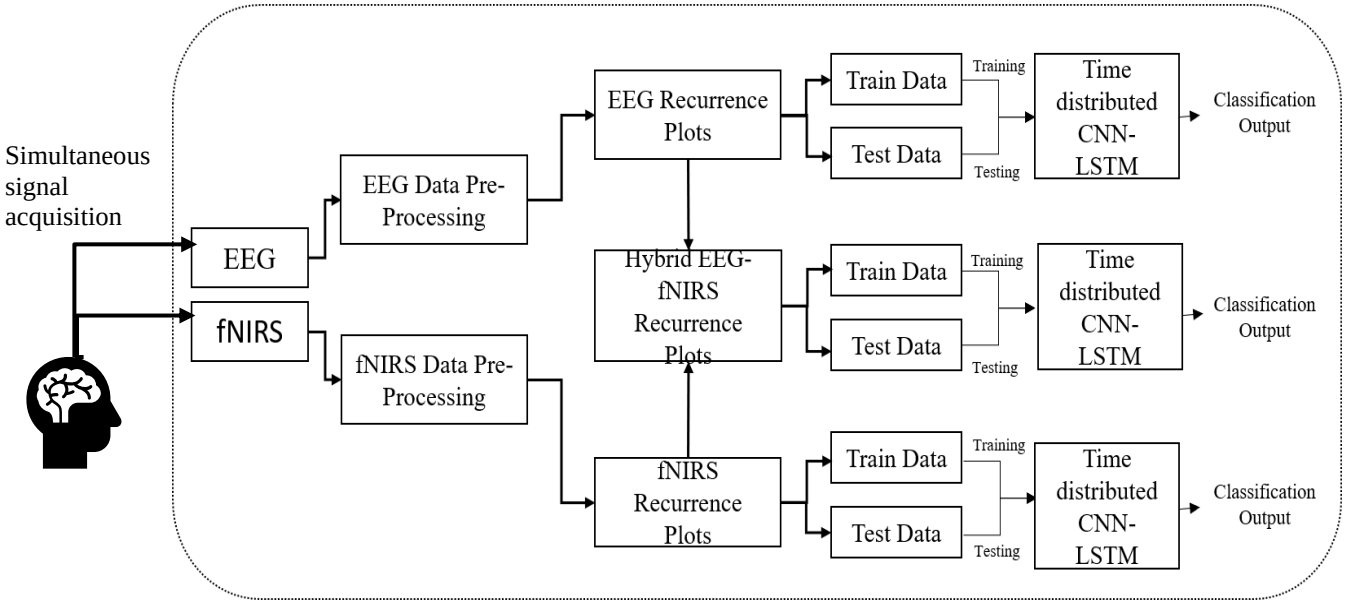

Figure 2-1: Methodology of Research

Each of the block shown in the above figure is discussed in detail in next sections of this chapter.

2.1 Dataset and Experiment Protocol

The research used an open source meta dataset. The data was recorded at the Technische Universität Berlin [15]. The data was acquired through 26 healthy participants. The data were

collected through three different paradigms, while the focus of attention was paid to the cognitive tasks. the three datasets A, B, and C chosen for three different cognitive tasks were n-back, discrimination response, and word generation respectively. On these grounds, the selected dataset was an apt choice for the research in the domain of hybrid BCI.

2.1.1 Participants

The subject size of the study was 26. Twenty-six health individuals were employed in the study. The subjects were 9 males and 17 females, with ages ranging from 17 to 33 years. The exclusion criteria were any previous history of the neural or psychological disease. The experimental procedure was well communicated with the subjects before the data collection. The written consent of the subjects was also taken.

2.1.2 Experimental Paradigm

It was ensured that the subjects sit in a comfortable chair with the armrests, the chair was faced towards a 24 inches LCD monitor. For each session of the data recording, it was ensured that the distance between the subject and the monitor is 1.2 meters. The subjects were asked to use the numeric pad with their index and middle fingers. The subjects were asked to press numeric keys 7 and 8. The keypad was set up on the right side of the arm of the chair. before data collection subjects were asked to keep their eyes focused on the monitor and avoid making unnecessary movements throughout the data acquisition, to avoid the motion artifacts. In each experiment, the subject was asked to perform three sessions of -back, DSR, and WG. Since the strain on the subject's focus was probable, owing to the long duration of data recording. Keeping this in view the subjects were asked to perform the activities in descending order concerning task difficulty. First task A was performed then C and lastly B.

In this study only dataset A (n-back) is used so only it is explained in detail in next section. One may refer to the paper for further details of other datasets and analysis.

2.1.2.1 n-back Dataset

The whole n-back dataset consists of total three sessions. Further, every single section consists of three series, namely 0-back, 2-back and 3-back tasks. the repetition series in a section is in a counter-balanced order.

Thus, for every single patient total nine n-back series were performed. Total recording time of each series was 62 seconds, the initial 2 seconds were dedicated to the task illustration, the following 40 seconds were reserved for the task performance, and the last 20 seconds were of the rest period. However, additional assistance was provided to keep the subject focused. The starting and ending of the task was signaled by a 250 ms beep, with the visual of 'STOP' was presented at the end of the task on the screen. The rest phase was signified with a fixation cross on the screen. The task period was of two seconds, any random digit was displayed on the screen. Each number in a trial was presented for 0.5 seconds, followed by a cross to focus on the screen, which stayed on the screen for the rest of the duration. Twenty such trails were repeated. The target used to appear with a 30% chance. In the first task, namely the 0-back task the subjects were made to press either the targeted key or the non-targeted key on the numeric keypad. The participants were asked to press the targeted key using the right index finger and likewise the non-target key with the middle finger of the right hand. The 0-back task was followed by the 2 and 3 back tasks. in these tasks, the subjects were asked to press the target button only in the case that if the number being displayed matches the 2 and 3 prior numbers. The task period was followed by the fixation cross, the subjects were instructed to gaze at the cross and relax. This allowed the brain state to return to the normal baseline value.

Thus, for every single n-task, there were a total of 180 trials. As there were 3 sessions, each having three series, while every single series encompassed 20 trials, making a total of 180 trials. Experiment protocol for n-back dataset is shown in Figure 2-2.

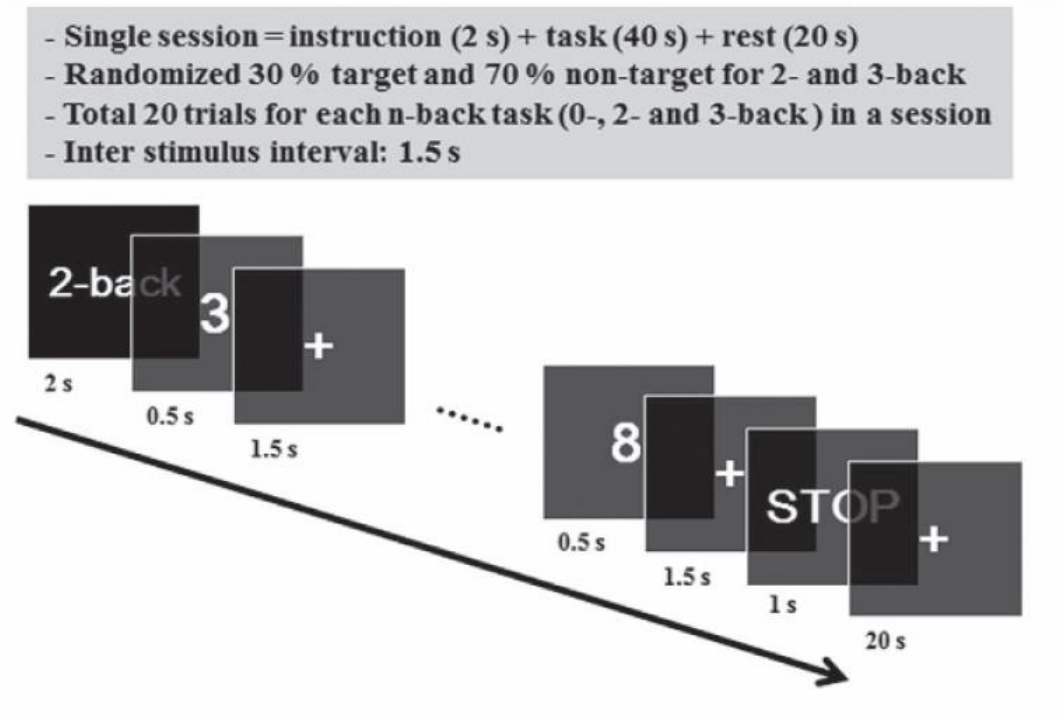

Figure 2-2: Experiment protocol on n-back dataset

2.1.4 Data Acquisition

The EEG and fNIRS data were recorded simultaneously, to keep the data synchronized a parallel port was used to send the triggers.

Sampling frequency of EEG data was 1000 Hz. The BrainAmp EEG amplifier was used by the vendors. A stretchy fabric cap was used to place the active electrodes. Thirty electrodes were used for acquiring the data. The electrodes were placed according to the internationally recognized 10-5 system [41]. The electrodes were placed at frontal (Fp1 to FC6), motor cortex (Cz to CP6) and parietal region (Pz to POz) and occipital region (O1, O2) TP9 was kept as a reference while the TP10 was made ground. To determine the Electrooculogram signal (EOG) an EEG amplifier was also used. The EOG was recorded using four surface electrodes where 2 horizontal electrodes were placed at the canthus of the eye while the vertical electrodes were placed above and below the right eye. the sampling rate of the EOG signal was the same as the EEG.

The fNIRS data were recorded at 10.4 Hz sampling frequency via the NIRScout by NIRx Medizintechnik GmbH, Berlin, Germany. Sixteen electrodes, combination of sources with detectors were positioned at the frontal lobe across the region of AFz to AF8, four channels were

paced at C3 and C4 for the motor cortex region. four channels were places in the parietal region across P3 and P4. Likewise, four channels around the POz region for the occipital region. The distance between the source and the detectors was ensured to be 30mm [42-44]. The Optodes of the NIRS were fixed with the EEG electrodes on the same cap. The positioning of the electrodes and the Optodes have been illustrated in figure 1-3. Yellow circles reflect the positioning of the EEG electrodes while the red circles showed the NIRS Optodes.

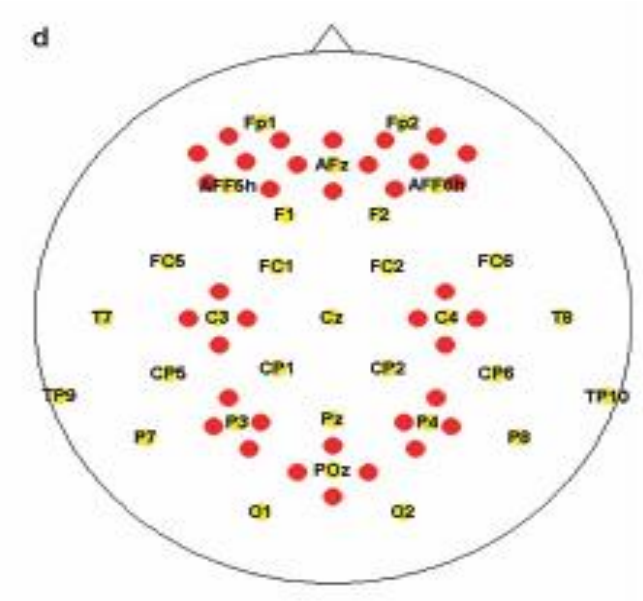

Figure 2-3: Electrode placement for simultaneous data acquisition of EEG and fNIRS according to 10-20 electrode placement system (red = fNIRS, yellow = EEG)

2.1.5 Data Pre-processing and Labelling

The EEG data were down sampled to 200Hz. For filtering purposes, a 6th order Butterworth bandpass filter was used. The passband frequency range of the filter was 1-40 Hz. To pre-process the fNIRS data, the acquired data were first translated to the oxy and deoxy-hemoglobin intensity variations. The conversions were made through the modified Beer-Lambert law. The fNIRS raw data were down sampled at 10Hz. The fundamental frequency of this dataset was very low so the down sampled was not fed into the Butterworth bandpass filter owing to the reason that the fundamental frequency was low. The data was instead low pass filtered to avoid the loss of the fundamental frequency component. The cutoff frequency of the filter was chosen to be 0.2 Hz.

The data was acquired through MATLAB R2013b. however, further processing was done using python on Spyder in the anaconda development environment. The dataset after filtration was labelled using the activity time markers given with the acquired continuous EEG and fNIRS signals. Four classes i.e., three n-back classes, 0-,2- and 3-back and one of the rests, were labelled w.r.t to the experiment protocol. The labelled data was then sent to the RP function for RP construction.

2.2 Recurrence Plots

A recurrence plot is a contemporary technique for analyzing nonlinear data. recurrence lots are a technique that employs the visualization of a square matrix. The elements of the matrix link to the dynamic state repetition. The ordered pair of the matrix corresponds to the specific pair of the timing of the repetition.

The recurrence analysis is a graphical technique that aims to point towards the hidden recurring patterns (Eckmann et al., 1987). Let us illustrate this by supposing that our desired information is univariate time series data. The data under analysis is a subpart of the large n-dimensional dataset. In the case of the above-mentioned scenario, Taken presents the viewpoint that the topological picture of this original n-dimensional dataset can be made by using a single observable variable.

Thus, the embedded matrix namely the x^m can be constructed as:

$$x^m_i = (x_i, x_{i+d}, x_{i+2d}, \ldots, x_{i+(m-1)d})$$

where xi is the scalar series, dimension is represented with m while d is signifying the delay. In case:

$$\mathbf{m \geq 2n + 1}$$

above mentioned condition satisfies then the single output variable exhibits the potential to recreate the whole system. the recreation heavily depends upon the sequence of the embedded matrix. The sequence can be vigilantly controlled by aptly choosing the parameters m and d.
asymmetric matrix of the Euclidean distances can also be constructed by measuring the distance between the pairs of the embedded vectors. In the recurrence plots, these distances are translated into an equivalent color, each distance has a distinctive color. Thus, in other words a recurrence

plot is a rectangular assortment of the pixels whose color depends upon the corresponding magnitude of the values. The coordinates of the pixels also carry useful information that is linearly related to the location of that data into the original data matrix.

The use of ε is also commonly employed in the recurrence plots this ε. I referred to it as the critical radius. Each value is compared with the critical radius if the pixel value is less than or it is equal to ε only then the pixel is displayed as a darkened pixel. In other words, RP is a visualization of a square recurrence matrix showing all the instances of times at which a state of a nonlinear system repeats where columns and axis of recurrence matrix correspond to specific time intervals. In technical terms, an RP shows all the times of a nonlinear time signal from a dynamical system when its phase space trajectory visits approximately the same area in the phase space. In graphical terms, it is a graph of

$$\vec{x}(i) \approx \vec{x}(j)$$

where i is on a horizontal axis and j is on a vertical axis, and $\vec{x}$ is a phase space trajectory of the dynamical system. Thus, I constructed a binary recurrence matrix using a certain time window w = 5 sec where any two-time steps are separated by the time interval ε = 0.1 and step size of 10 as follows:

$$R(i, j) = \begin{cases} \mathbf{1} \ \boldsymbol{if} \ \|\vec{x}(i) - \vec{x}(j)\| \leq \boldsymbol{\varepsilon} \\ \mathbf{0} \qquad\qquad \boldsymbol{otherwise}, \end{cases}$$

where i and j are horizontal and vertical time axis, $i, j \in \{t_0, t_1, \ldots . \mathrm{t}, \ldots t_T\}$. The recurrence plot is a visualization of the recurrence matrix with a black little square of the lattice at coordinates (i, j) if $R(i, j) = 1$, and a white little square if $R(i, j) = 0$.

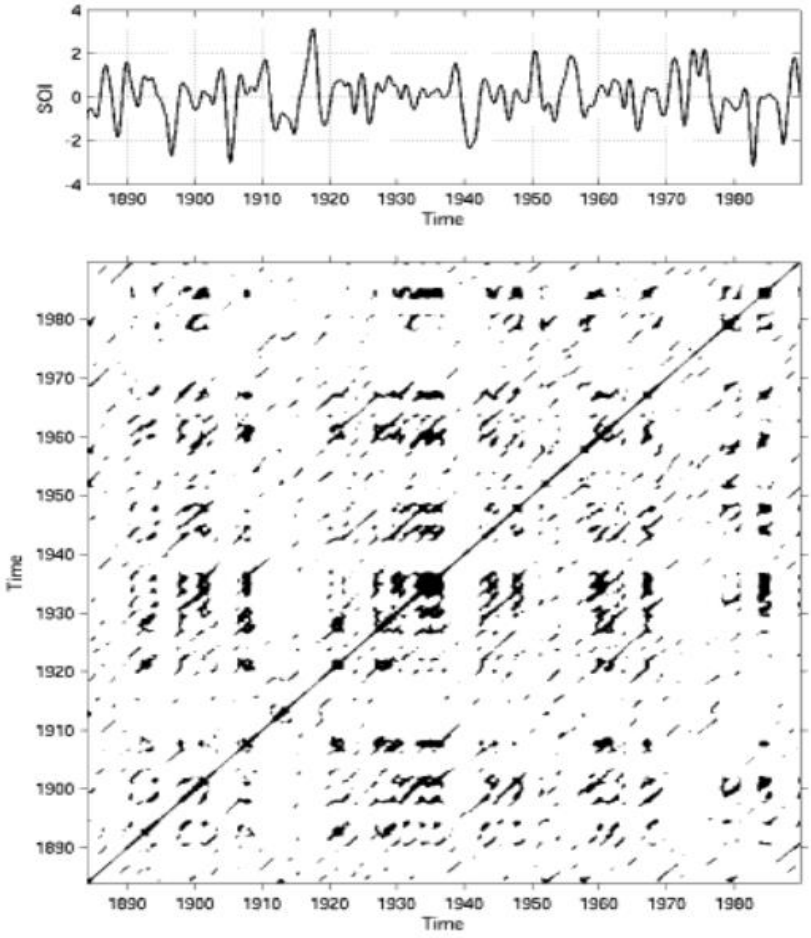

Figure 2-4: Recurrence plot of a time signal.

Operationally the plot is drawn as follows:

a) A certain time window $\vec{\omega} = \ < t_0,\ t_1, \ldots . \mathrm{t}, \ldots t_T >$ is chosen where any two-time steps are separated by the time interval ε, and where the state $\vec{x}(t)$ of the system is recorded for each time step, thus collecting the trajectory X= $< \vec{x}(t_0),\ \vec{x}(t_1), \ldots \vec{x}(t_T) >$.

b) A 2D plot is created where the x-axis and y-axis both report $\vec{\omega}$, forming a $T \times T$ lattice of little squares each with side measuring ε.

c) The X are used to compute a matrix $D\ (T, T)$ formed by binary elements recording the recurrence/non-recurrence of values $\vec{x}$ through the binary function:

$$\boldsymbol{R}\ (\boldsymbol{i},\ \boldsymbol{j}) = \begin{cases} \mathbf{1}\ \boldsymbol{if}\ \ \|\vec{\boldsymbol{x}}(\boldsymbol{i})\ - \vec{\boldsymbol{x}}(\boldsymbol{j})\| \ \leq \boldsymbol{\varepsilon} \\ \mathbf{0} \qquad\qquad\qquad\quad \boldsymbol{otherwise}, \end{cases}$$

where $i, j\ \in \{t_0,\ t_1, \ldots . \mathrm{t}, \ldots t_T\}$.

d) The recurrence plot then visualizes $D(T, T)$ with a black little square of the lattice at coordinates (i, j) if $R(i, j) = 1$, and a white little square if $R(i, j) = 0$.

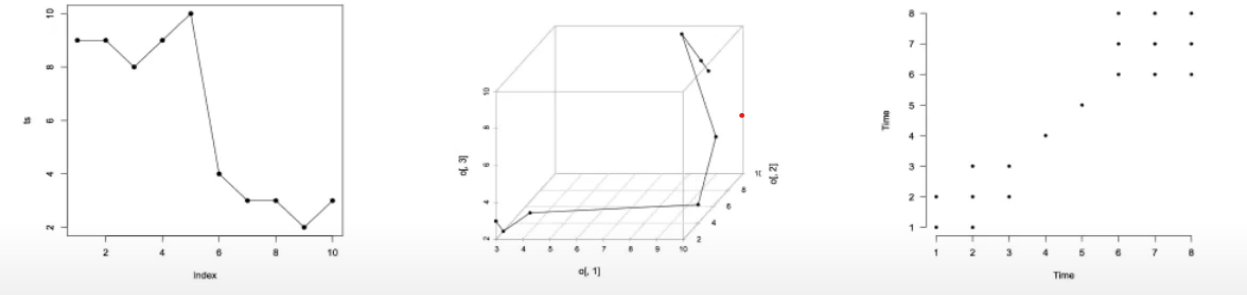

Figure 2-5: Steps of recurrence plot formation

2.3 Classification Network

2.3.1 Convolutional Neural Networks (CNN)

CNN is a multi-layered neural network with architecture to detect the complex features in the data. Unlike the traditional multi-layer perceptron architectures, CNN uses two operations called 'convolution' and 'pooling' to reduce the image into its essential features, and then uses

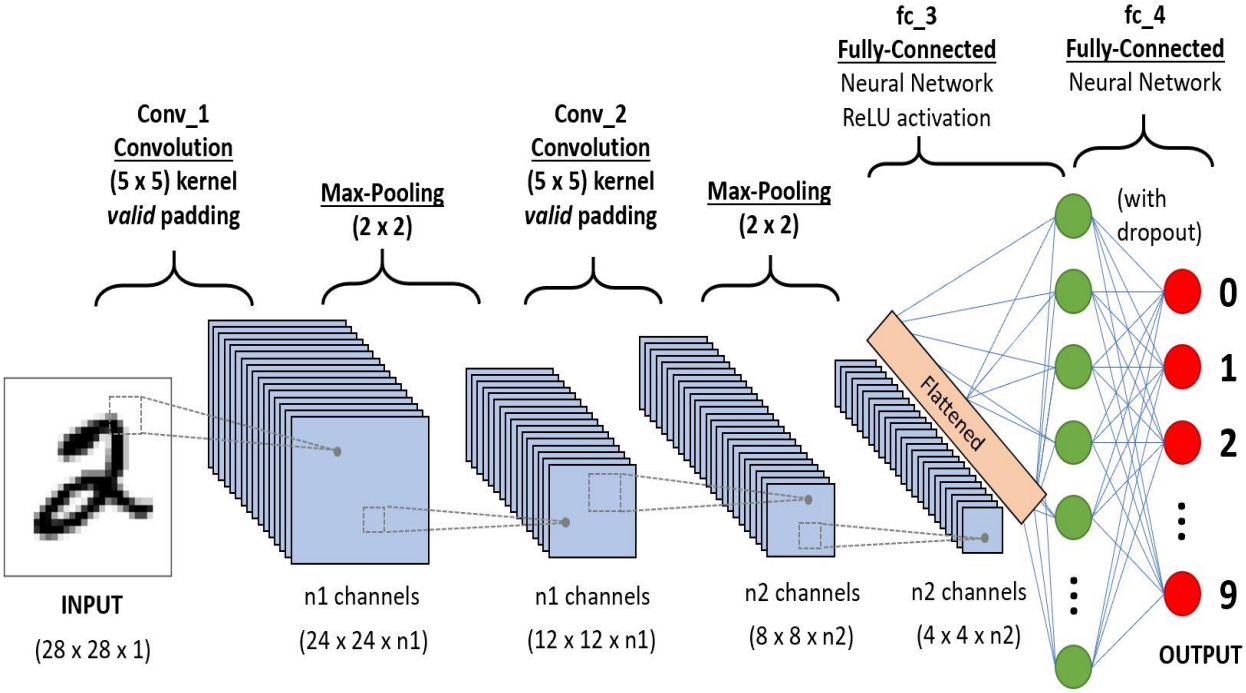

Figure 2-6: Architecture of convolutional neural networks

those features for understanding and classification of the image. CNNs are made up of some basic building blocks. Typical CNN architecture is shown in figure:

These blocks include Convolutional Layer in which a filter or kernel is passed over an image, Activation Layer has normally an activation function "Relu", this layer introduces nonlinearity that allows the network to train itself through backpropagation. Pooling layer down-samples and reduces the size of the matrix, it focuses on the most prominent information in each feature of the image. The last one is named the fully connected layer, this layer outputs the different probabilities associated with every label attached to the image. The label with the highest probability is the classification decision. CNNs are widely used in agriculture, self-driving vehicles, healthcare, and surveillance. The output size of every layer of CNN is determined with:

$$Output\ size\ (W, H) = \frac{(N - F)}{Stride} + 1$$

Where W and H are the width and height of the output activation map or feature map, N is the dimension of the input activation or feature map, F is dimension of filter sliding over the input image or activation map, stride is the number of steps taken whille sliding filter. While the parameters of a layer are calculated using:

$$Parameters = (\mathrm{W} * \mathrm{H} * \mathrm{K}) + \mathrm{K\,biases}$$

Where W and H are the width and height of the output activation map or feature map, K is the number of filters and K biases are the number of biases.

2.3.2 Long-Short-Term Memory (LSTM)

LSTM or long-short-term memory networks are the type of Recurrent Neural Networks that uses some special unit in addition to the standard units. These special units include the "memory cell" that maintains information in its memory for a longer period. LSTM has feedback connections unlike the standard feed-forward neural networks, it can process the whole sequence of data i.e., speech, video, etc. LSTM is used widely in speech recognition, handwriting recognition, handwriting generation, Music generation, Language translation, image captioning, and anomaly detection in intrusion detection systems. A simple LSTM unit is made up of a cell, input gate, output gate, and forget gate. The cell remembers the information whereas gates regulate the flow of information. LSTM networks are modified forms of RNN, they remember the past data in memory. The logistic sigmoid function for the LSTM memory cell is given by:

$$f(x) = \frac{1}{1 + e^{-k(x-x_0)}}$$

Where:

e is the natural logarithm base,

x0 is the sigmoid midpoint,

K is the logistic growth rate.

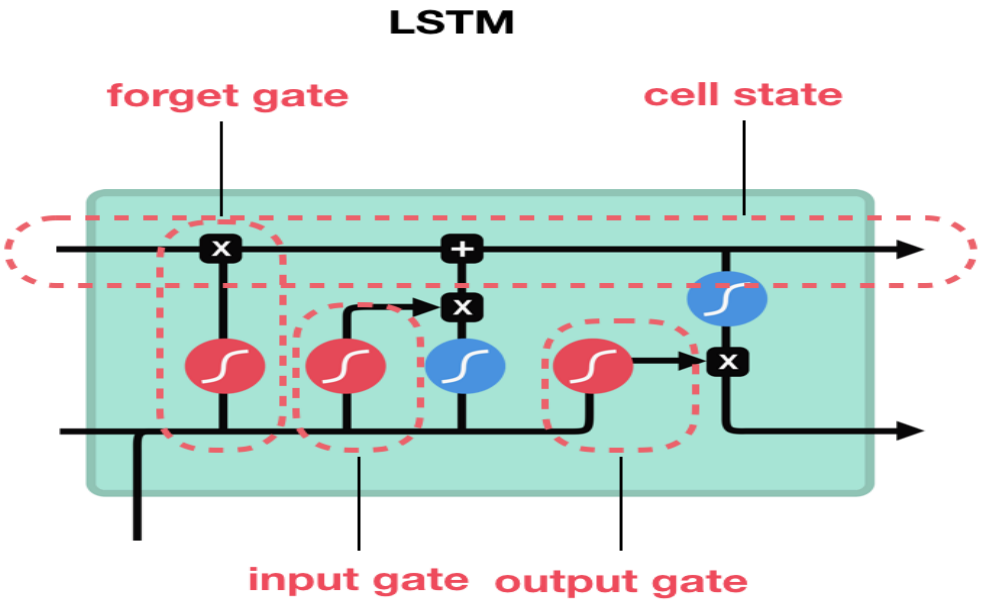

Figure 2-7: Architecture of a Memory Cell of Long Short Term Memory Network

In LSTM gates outputs are determined by:

$$\text{Input activation:} \quad a_t = \tanh(W_a \cdot x_t + U_a \cdot out_{t-1} + b_a)$$

$$\text{Input gate:} \quad i_t = \sigma(W_i \cdot x_t + U_i \cdot out_{t-1} + b_i)$$

$$\text{Forget gate:} \quad f_t = \sigma(W_f \cdot x_t + U_f \cdot out_{t-1} + b_f)$$

$$\text{Output gate:} \quad o_t = \sigma(W_o \cdot x_t + U_o \cdot out_{t-1} + b_o)$$

Which leads to:

Internal state:

$$state_t = a_t \odot i_t + f_t \odot state_{t-1}$$

Output:

$$out_t = \tanh(state_t) \odot o_t$$

For vectorized operations and ease to use we define them as:

$$gates_t = \begin{bmatrix} a_t \\ i_t \\ f_t \\ o_t \end{bmatrix}, \; W = \begin{bmatrix} W_a \\ W_i \\ W_f \\ W_o \end{bmatrix}, \; U = \begin{bmatrix} U_a \\ U_i \\ U_f \\ U_o \end{bmatrix}, \; b = \begin{bmatrix} b_a \\ b_i \\ b_f \\ b_o \end{bmatrix}$$

LSTM parameters are calculated as:

$$Parameters = 4 * ((output\_size + 1) * inputs + inputs\text{^}2)$$

2.3.3 Time Distribution Layers

In ML or DL, for classification problems we have to predict outputs on complex data like images etc. using neural networks. Taking example of CNN here, one needs to send multiple inputs one at a time to be analyzed. It is okay in case of classification problems related different events or objects but sometimes, the inputs are chronological. Like in my case activity and rest data of EEG or fNIRS is chronological i.e., events are happening in a sequence not randomly. In such cases traditionally two solutions are opted as shown in figure 2-8.

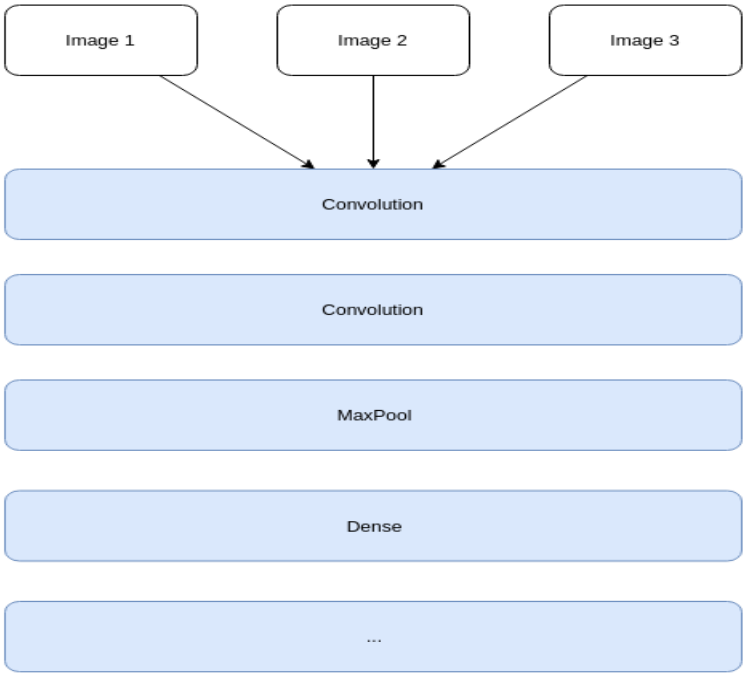

Figure 2-8: Convolutional neural network with input sequence

The first problem that usually arises while feeding multiple images in CNN at a time, that typically takes one image at a time, using these approaches is it will cause unwanted image merging. In typical sequential neural networks layers are fully connected means every layer has impact on all layers forward and backward to the input. It is okay in case of one image but while dealing with multiple images, it will cause unwanted merging of image pixels within several images. Figure 2-9 shows the solution to the above-mentioned problem.

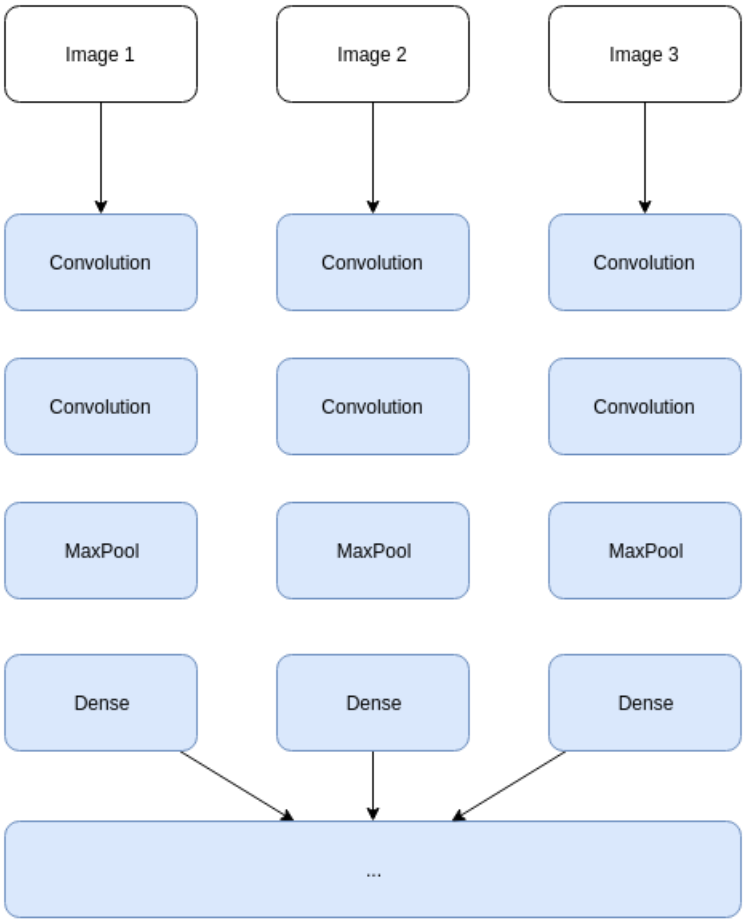

Figure 2-9: Desired Convolutional neural network with input sequence

In this case each image has got its own convolutional flow i.e., the input images will not merge as desired but it is like one CNN per image. This will cause several unwanted behaviors. First, very long training time will be required as there are multiple convolutions to do and train each network separately. Secondly, each convolutional flow will have separate set of weights, for one sequence, so there will be different features detection that will not be linked with each other.

Lastly based on the image sequences, different CNN will detect different features that the other network is not doing may be. Here, time distribution layers make up the best solution as time distributed layers apply the same layer to several inputs and it produce one output per input to get the result in time. Moreover, the weights are shared and do not need separate updating for each input in backpropagation, thus it saves time and computation as well.

Now, time distribution layers when used with CNN and LSTM, there are two possible configurations to implement them in the network. They can be used either before or after LSTM layer depending on the application.

Figure 2-10 shows the configuration of time distributional layers before LSTM. It will first use the CNN network to extract features from an input sequence and then will use the memory power of LSTM to chronologically order the input sequence and detect the movement or direction or any activity. So, this configuration is used when the demand for application is to learn or extract some features first and then based on the extracted feature, order them with LSTM and detect any activity, like in this study. So, this configuration will be used latter in this work.

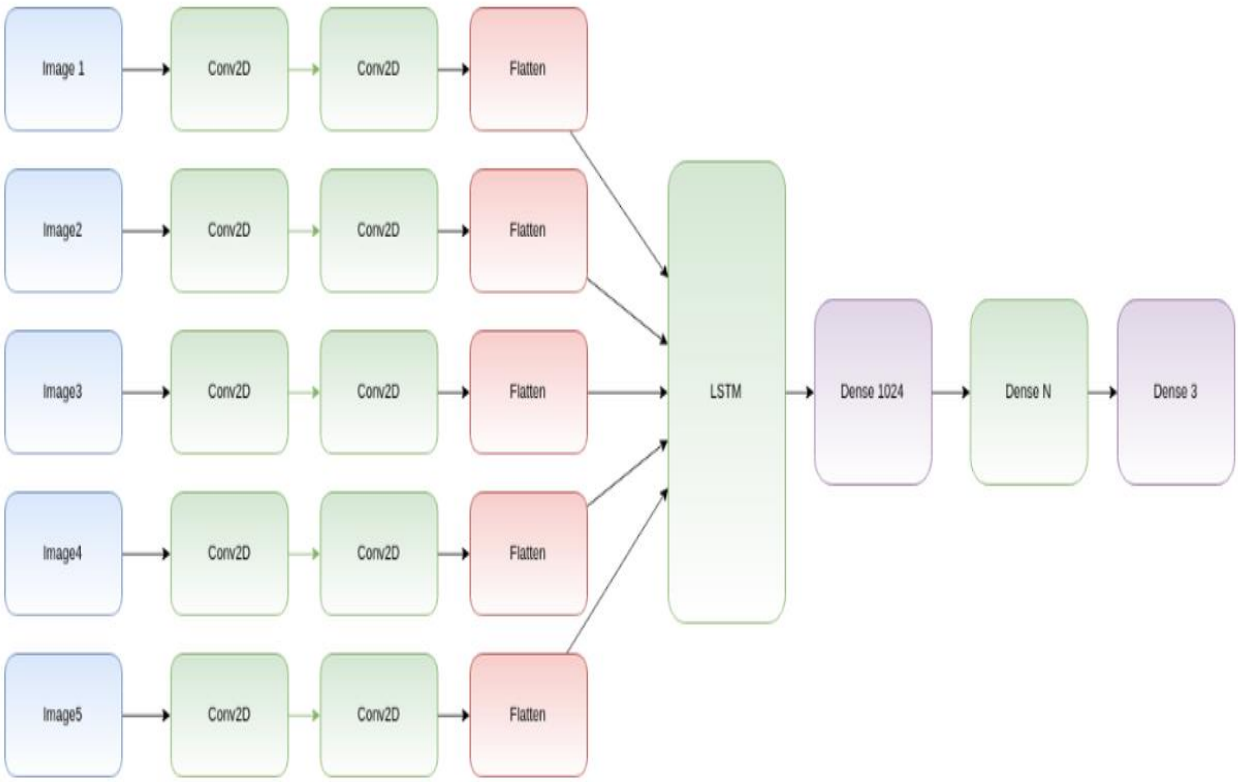

Figure 2-10: Time distributed before LSTM

This is just the representation for each input, same convolutional and flatten layers will be used.

Figure 2-11 shows the second possible configuration for time distributional layers with CNN and LSTM i.e., using time distributional layers before LSTM. This configuration is useful when one needs LSTM to produce a sequence and then CNN to extract features from that sequence. Here LSTM is working not only as a filter, but it is also keeping input computations in the memory so that one can retrieve them to make manipulation.

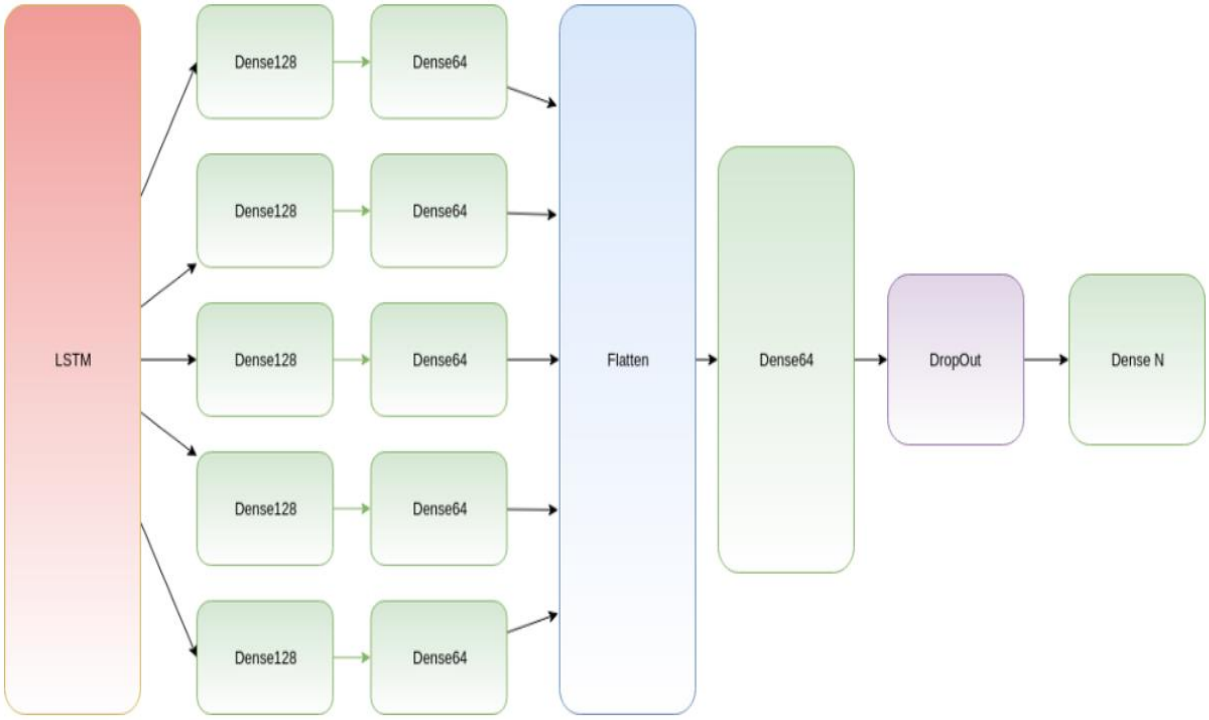

Figure 2-11: Time distributes after LSTM

This is just the representation for each input, same convolutional and flatten layers will be used.

2.3.4 Time Distributed CNN-LSTM

Over the period, researchers have experimented with different architectures and types of deep learning networks. Unlike images, text, voice, and other widely used types of datasets, neuroimaging signals are intrinsically different and possess important chronological order in themselves. This chronological order dictates the flow of necessary information to detect activity or action. The examples of such chronological order might be the initial dip at the start of activity in fNIRS signals and positive deflection in event-related potential (ERP) P300 signal in EEG. A novel CNN-LSTM network is designed for this study. The network consists of one CNN and one LSTM module combined with a Dense layer. The data after pre-processing is fed into the CNN module which consists of two convolutional layers each having 16 filters and 'relu' as an activation function and one max pooling layer. The CNNs are best known for their feature extraction abilities from 2-3D images. As we are working on the sequence of the data in form of time windows that are chronologically ordered, we want to be able to detect relations from window to window in a given input. Now to enable the network to use memory and enhance its prediction, the LSTM layer is used. The convoluted output from the CNN block is reshaped and flattened before feeding into the LSTM layer. The layers up till LSTM layers are wrapped inside a time-distributed layer that allows applying these layers to every temporal slice of an input data. This time-distributed wrapper applies the same instance of convolutional layers to each of the timestamps, so the same set of weights are used at each timestamp. The LSTM layer after passing through another dense layer terminates into the Output layer.

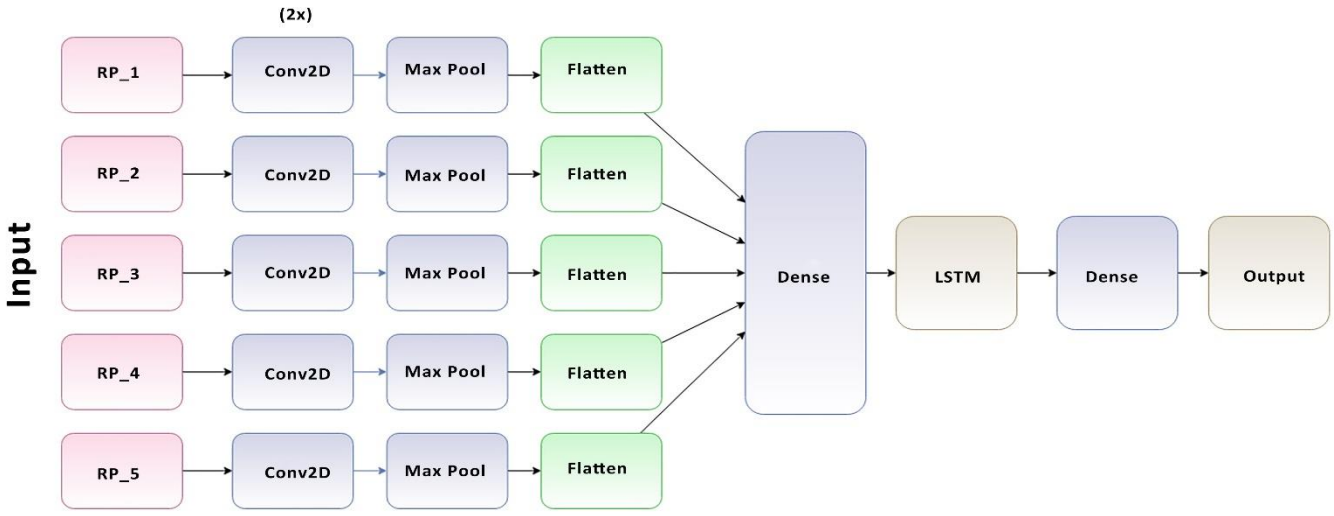

Figure 2-12: Time distributed CNN-LSTM network for 4-class EEG and fNIRS classification

To the best of the authors' knowledge, no one has exploited this chronological order using time-distributed layers in deep learning models. The constructed RPs with fixed window length and overlapping portion are fed into the network as images. The different configurations of this proposed network for fNIRS, EEG, and hybrid modalities are discussed in detail in the Discussion section. The network architecture for EEG and fNIRS BCI is given in figure.

For hybrid BCI, almost same architecture is used except that now instead of a single modality's RPs, RPs for both EEG and fNIRS are being fed into the network in parallel order. As with a unit increase in data points, size of RPs grows exponentially and EEG's sampling frequency is higher than the fNIRS, it is still wrapped in time-distributional layers while fNIRS RPs are passed through a separate network and the hybrid feature extracted from both modalities are combined at the dense layer for further classification.

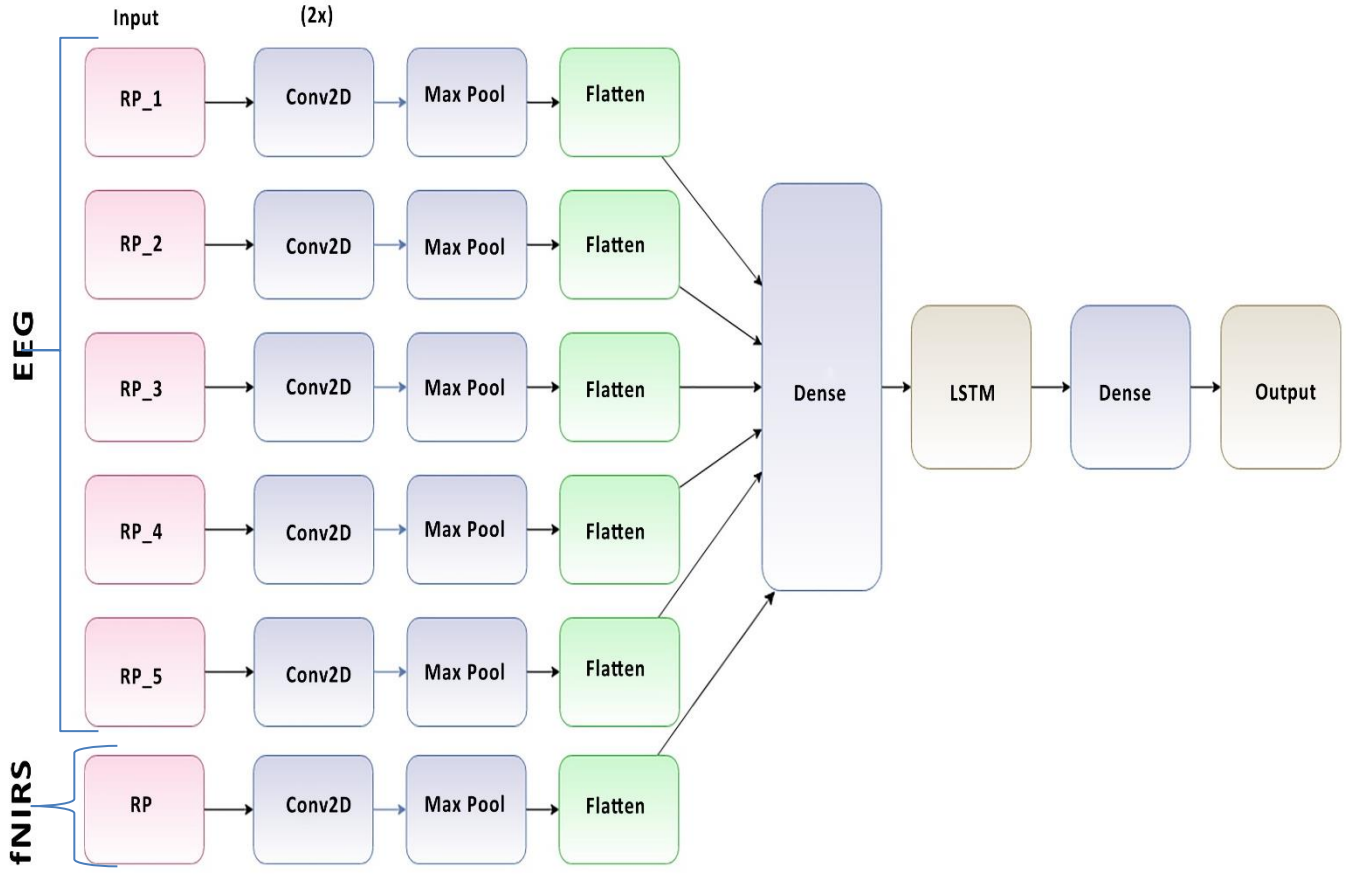

Figure 2-13: Time distributed CNN-LSTM network for 4-class hybrid EEG-fNIRS classification

Researchers have put a tremendous amount of effort into determining the single best architecture for the deep learning neural network. This gives rise to the standalone sub-research field known as Neural Architecture Search (NAS). But as of yet, unfortunately, there is no definite answer for the optimal neural architecture priori. The number of neurons, the number of filters, the number of layers, their combinations, dropout, and max-pooling percentage, etc, all remain to be at best 'hyper parameters'. The most viable approach seems to be using own intuition and domain knowledge and start with a rough guess for these parameters and iteratively shortlist to the good working parameters. In this study, the design process for the NAS was as follows: create a network with a minimum number of parameters, a single conv layer, a single LSTM layer, and one dense layer, then tune other hyperparameters. Add more layers and then tune network hyperparameters with grid search using the sklearn wrapper. We performed the above grid search with a sample of data and choose the best performing network for EEG, fNIRS, and EEG+fNIRS datasets. However, the issue with this approach was input dimensions mismatch due to the extra amount of features in the hybrid dataset as compared to the single modality datasets. This, problem is solved by adding another sequence module on top of the EEG network architecture and wrapped it inside the TD layer just like EEG one. The later stages of a network like dense layer, LSTM layer, and following layers remain the same but this solves the input dimensionality mismatch problem.
The modal parameters summary is given in figure.

Layer (type)	Output Shape	Param #
time_distributed_1 (TimeDist	(None, 1, 148, 148, 16)	160
time_distributed_2 (TimeDist	(None, 1, 146, 146, 16)	2320
time_distributed_3 (TimeDist	(None, 1, 73, 73, 16)	0
time_distributed_4 (TimeDist	(None, 1, 85264)	0
time_distributed_5 (TimeDist	(None, 1, 32)	2728480
lstm_1 (LSTM)	(None, 512)	1116160
dense_2 (Dense)	(None, 256)	131328
dense_3 (Dense)	(None, 4)	1028

Total params: 3,979,476
Trainable params: 3,979,476
Non-trainable params: 0

Figure 2-14: Modal parameters summary

The modal summery is shown in figure.

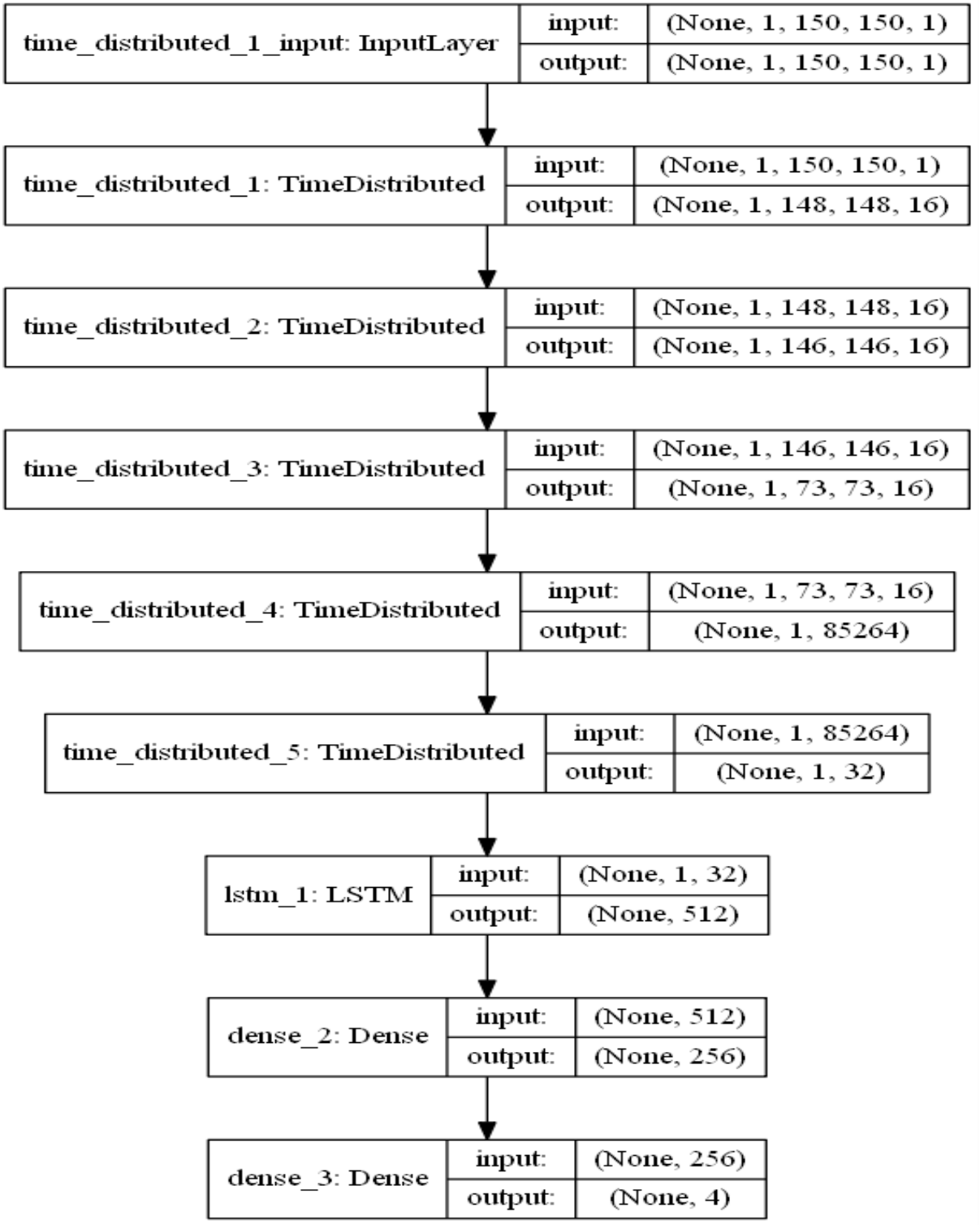

Figure 2-15: Modal summary(layers, input and output sizes)

CHAPTER 3: RESULTS

The time-distributed CNN-LSTM is used in this research to classify 4-classes i.e., three n-back activity and the rest using the simultaneously acquired EEG-fNIRS dataset for 26 subjects. Fig. 1 depicts the non-linear mapping of acquired brain signals to the new dimension. Each subject data is split into 70:30 ratio as train and test set before performing classification to avoid over-fitting and for better generalization. The average accuracy achieved for 4-class classification with fNIRS is 78.08%, EEG is 80.10% and hybrid EEG-fNIRS data is 83.65%. While the maximum accuracy is 86.23%, 88.70% and 92.31%, respectively. The deep learning algorithms are trained on a GTX 1060 graphic card having 3 GB VRAM and Intel 6th Gen Core i7-6700HQ processor with 3.2 GHz frequency. The Keras API is used with the TensorFlow backend on Spyder in Anaconda integrated development environment. Table 3-1 summarizes the results of 22 participants in terms of their classification accuracies in percentages.

Table 3-1: Accuracies of fNIRS-BCI, EEG-BCI and Hybrid EEG-fNIRS-BCI

Subject No.	**Accuracies of fNIRS BCI (%)**	**Accuracies of EEG BCI (%)**	**Accuracies of Hybrid EEG-fNIRS BCI (%)**
1	76.45	77.68	81.66
2	76.73	78.79	82.49
3	83.33	85.97	89.48
4	79.27	80.76	84.70
5	70.34	73.00	76.58
6	81.11	83.61	86.99
7	79.47	81.82	84.77

8	79.99	82.14	85.52
9	86.23	88.70	92.31
10	68.78	70.97	74.83
11	75.45	77.69	81.17
12	79.12	80.99	84.68
13	72.18	73.85	77.36
14	83.79	86.54	89.44
15	79.50	81.13	84.89
16	86.09	87.63	91.37
17	79.86	81.63	84.82
18	77.64	79.84	83.44
19	74.83	76.10	79.97
20	83.42	84.81	88.66
21	65.06	67.37	70.74
22	79.00	81.19	84.53
….			
Maximum accuracy	85.9	88.10	92.4
Average accuracy	79.7	83.6	88.5

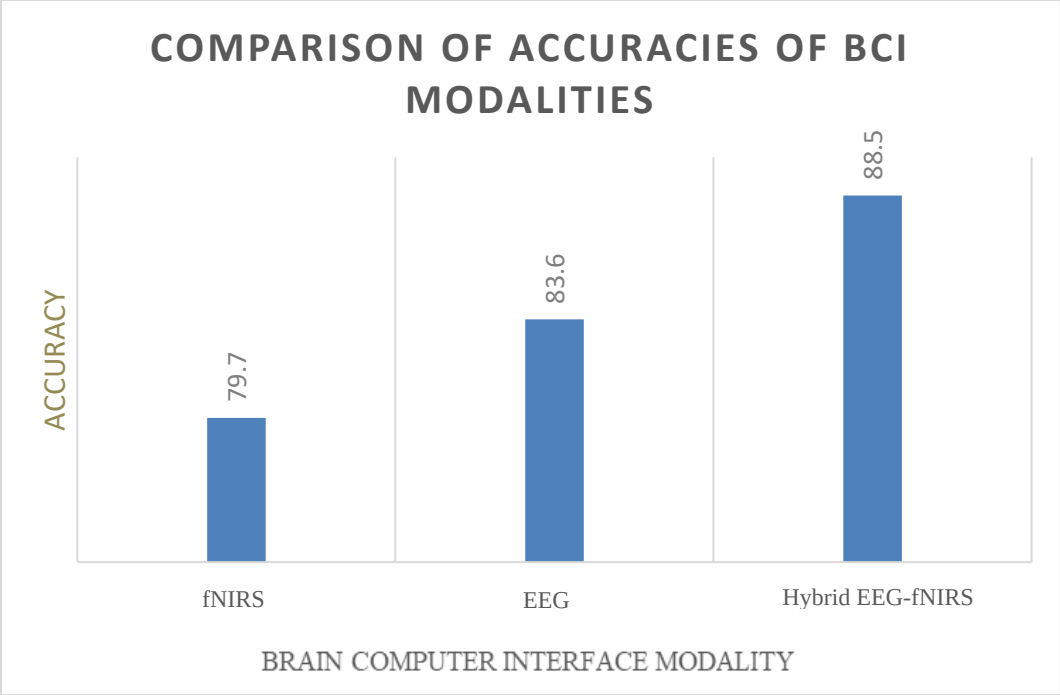

Figure 3-1: Comparison of accuracies

CHAPTER 4: CONCLUSIONS AND FUTURE WORK

Researchers highly appreciate the low-cost neuroimaging modalities. The modalities which offer the non-laboratory setup convenience usually are the choice of interest too. The most commonly used neuroimaging modalities in this respect are EEG and fNIRS. Both the modalities are portable as well as low cost as compared to the others. However, EEG does not have a good spatial resolution. The spatial resolution is approximately around 10mm [11],[15]. The contrasting comparison of the temporal and spatial resolution manifests the tradeoffs while using the EEG modality. In contrast to the EEG, fNIRS constructs the functional neuroimages of the brain by employing near-infrared light. Since fNIRS measures the hemodynamic responses, so it is bind with an innate delay in the measurement [5]. Various methods have been offered in this regard to compensate for this conducive slow command generation. EEG and fNIRS hybrid can too compensate for the delayed response of the fNIRS modality. But the sampling frequencies of both modalities are different resulting in information loss. Moreover, the most important objective of all studies carried on BCI is to enhance real-time classification accuracies and reduce computational costs, with multiple commands, emphasizing the need to develop appropriate identification and classification methods for real-time BCI [7]. Usually, multichannel brain signal acquisition modality i.e., EEG, is used to analyze brain motor activity by different existing methods like time and frequency feature analysis, event-related synchronization-desynchronization analysis, common spatial or temporal patterns, and spatial-spectral decomposition. The back draw of many of these methods is they require high computational costs, thus less feasible to use for real-time BCI [8].

To solve the above problems, I have used RPs as a pre-processing step. One advantage of using RP with neural network is it incorporates the whole signals and does not require any extra steps to make hybrid modalities compatible for each other. Moreover, it also minimizes any feature extraction of pre-processing steps like finding temporal or spatial features etc. The constructed RPs of EEG, fNIRS are then fed to the classification network to detect the class of activity (0-, 2-, 3-back or rest) . The classification network used is time-distributed CNN-LSTM. CNNs are best known for feature extraction from multi-dimensional images. While the recurrent neural network has an excellent ability of pattern recognition in sequences of input. But they have stability issues either due to exploding gradients or vanishing gradients. I used a variant of recurrent neural

network that solved the exploding and vanishing gradient problem by using memory cells, Long Short-Term Memory (LSTM). The highest classification accuracy of four class mental workload data for the brain-computer interface is achieved using this network. Moreover, the implementation of time distributional layers has made the computation not only easy but faster. This is indeed a state-of-the-art algorithm in the present brain-computer interface realm. This makes them an excellent choice as the network do not require a long time for training. Also, it has in order of magnitude fewer parameters. That can be used in real-time BCI. There are a lot of potential applications for recurrence plots in BCI. Working in that direction will help researchers to mitigate nuances attached to deep learning algorithms in BCI.

APPENDIX A

Table-I

Visual evoked nerve cerebral oxygen characteristics analysis based on NIRS-EEG				
2018	Hybrid NIRS-EEG	Relation between electrophysiological And hemodynamic responses to a checkerboard stimulus reversing.	1) mBLL for detecting cerebral oxygenation concentration using NIRS. 2) SSVEP signal detection using EEG through time and frequency domain analysis. Amplitude detection of P100N135. 3) Linear regression analysis to find the relationship.	Results show that there is a linear relationship between P100N135 amplitude and cerebral Oxygenation concentrations in the visual cortex, positive association between the amplitude of the P100N135-component and HbO2 concentration changes and a negative correlation association between the P100N135-component amplitude and HbR concentration changes.
A hybrid NIRS-EEG system for self-paced brain-computer interface with online motor imagery				
2014	Hybrid NIRS-EEG	Designed a unique sensor frame that records NIRS and EEG simultaneously for the realization of system. a novel analysis method that detects the the occurrence of motor imagery with the NIRS system and classifies its type with the EEG system.	1) mBLL for detecting cerebral oxygenation concentration using NIRS. 2) Thresholding to detect motor imagery from NIRS signal. 3) Calculation of log-scaled variance, the alpha-band power, the beta-band power, the delta-band power and the theta-band power from 2D EEG signal. 4) Linear-SVM classifier for classification of left- or right-hand motor imagery.	An online experiment demonstrated that the hybrid system had a true positive rate of about 88%, a false positive rate of 7% with an average response time of 10.36 s.
NIRS-EEG joint imaging during transcranial direct current stimulation: Online parameter estimation with an autoregressive model				
2016	Hybrid NIRS-EEG	Online resting-state spontaneous brain activation may be relevant to monitor tDCS neuromodulatory effects that can be measured using electroencephalography (EEG) in conjunction with near-infrared spectroscopy (NIRS).	Kalman Filter based online parameter estimation of an autoregressive (ARX) model to track the transient coupling relation between the changes in EEG power spectrum and NIRS signals during anodal tDCS (2 mA, 10 min) using a 4 × 1 ring high-definition montage.	The online ARX parameter estimation technique using the cross-correlation between log (base-10) transformed EEG band-power (0.5–11.25 Hz) and NIRS oxy-hemoglobin signal in the low frequency(≤0.1 Hz) range was shown in 5 healthy subjects to be sensitive to detect transient EEG-NIRS coupling changes in resting-state spontaneous brain

				activation during anodal tDCS. Conventional sliding window cross-correlation calculations suffer a fundamental problem in computing the phase relationship as the signal in the window is considered time-invariant and the choice of the window length and step size are subjective. Here, Kalman Filter based method allowed online ARX parameter estimation using time-varying signals that could capture transients in the coupling relationship between EEG and NIRS signals.
A Mobile, Modular, Multimodal Bio-signal Acquisition Architecture for Miniaturized EEG-NIRS-Based Hybrid BCI and Monitoring				
2017	Hybrid NIRS-EEG	Objective was to design such an instrument in a miniaturized, customizable, and wireless form.	The design and evaluation of a mobile, modular, multimodal bio-signal acquisition architecture (M3BA) based on a high-performance analog front-end optimized for biopotential acquisition, a microcontroller, and open-NIRS technology is presented.	The designed M3BA modules are very small configurable high-precision and low-noise modules (EEG input referred noise @ 500 SPS 1.39 μ Vpp, NIRS noise equivalent power NEP750 nm = 5.92pWpp, and NEP850 nm = 4.77pWpp) with full input linearity, Bluetooth, 3-D accelerometer, and low power consumption. They support flexible user-specified biopotential reference setups and wireless body area/sensor network scenarios.
Imagined Hand Clenching Force and Speed Modulate Brain Activity and Are Classified by NIRS Combined With EEG				
2017	Hybrid NIRS-EEG	Simultaneous acquisition of brain activity signals from the sensorimotor area using NIRS combined with EEG, imagined hand clenching force and speed modulation	1) Feature extraction for NIRS: HbD and HbO features for 24 channels from (0,10) sec were extracted. 2) To identify different levels of hand clenching force and speed motor imageries, the instantaneous amplitude (IA), instantaneous phase (IP), and instantaneous frequency (IF) of EEG signals were calculated and combined into a feature vector	1) HbO-HbD (60-69%) 2) IA-IP-IF (70-74%) 3) Combined (71-78%)

		of brain activity, as well as 6-class classification of these imagined motor parameters by NIRS-EEG were explored.	that was expected to enhance classification performance. 3) It was assumed that the main factor influencing NIRS and EEG was imagined force and speed of hand clenching. The influence factor involved six levels. 4) Six-class classifications were performed in the study (three levels of hand clenching force and three levels of hand clenching force motor imageries) using SVM.	
Hybrid EEG-NIRS based active command generation for quadcopter movement control				
2016	Hybrid NIRS-EEG	Four active commands are generated using hybrid electroencephalography (EEG) and functional near-infrared spectroscopy (fNIRS) for quadcopter control in online environment.	Linear discriminant analysis (LDA) was used for the offline classification of data. Power spectral density was used to detect the left-hand clenching and SSVEP. Peak and skewness were used for the detection of eye-movements. Signal mean and signal peak of ΔHbO was used as features for NIRS data classification. Ten-fold cross-validation was used for the estimation of classification accuracies. We also used combined EEG and fNIRS signals to generate the commands.	For three subjects. 1) Mental arithmetic (avg. 86.6%) 2) Left-clenching Imagery (avg. 78.1) 3) Eye- movement (avg. 86.9) 4) SSVEP (avg. 87.2)
Long-term Monitoring of NIRS and EEG Signals for Assessment of Daily Changes in Emotional Valence				
2018	Hybrid NIRS-EEG	The indices of frontal alpha asymmetry (FAA) obtained from electroencephalography (EEG) data in the resting state, laterality index at rest (LIR) from near infrared spectroscopy (NIRS) data and CVM are compared with BDI and STAI scores.	1) FAA acquired as average FAA during the resting state. 2) LIR, 2-channel, concentration changes in HbO during measurement of left and right PFCs. 3) CVM, average comfort vector, emotional valance and arousal vectors were calculated. 4) we evaluated the correlations between the self-reported inventories and the diagnostic markers.	In this experiment, BDI and STAI scores in the two subjects changed by approximately 10% in 3 to 5 weeks. For each subject, a correlation between the BDI score and FAA was found. However, the correlations require further analysis with sample data obtained over longer periods so that a regression model can be developed. These experimental results suggest that FAA, LIR, and emotional valence of CVM can be diagnostic markers for assessment of daily changes in emotional valence.
EEG-NIRS Based Assessment of Neurovascular Coupling During Anodal Transcranial Direct Current Stimulation - a Stroke Case Series				
2015	Hybrid NIRS-EEG	NIRS recorded changes in oxyhemoglobin (HbO2)	Hilbert-Huang transform-based assessment of neurovascular coupling.	The results of this case series show that anodal tDCS induces a local neurovascular response

		and deoxy-hemoglobin (Hb) concentrations during anodal tDCS-induced activation of the cortical region located under the electrode and in-between the light sources and detectors. Anodal tDCS-induced alterations in the underlying neuronal current generators were also captured with EEG. Then, a method for the assessment of NVC underlying the site of anodal tDCS was proposed.		which may be used for assessing regional neurovascular coupling (NVC) functionality. It was postulated that tDCS leads to rapid dynamic variations of the brain cell microenvironment that perturbs hemodynamic and electrophysiological responses.
Utilization of a combined EEG/NIRS system to predict driver drowsiness				
2017	Hybrid NIRS-EEG	In this study, a new approach is introduced, a combination of EEG and NIRS, to detect driver drowsiness. EEG, EOG, ECG and NIRS signals have been measured during a simulated driving task, in which subjects underwent both awake and drowsy states. The blinking rate, eye closure, heart rate, alpha and beta band power were used to identify subject's condition.	Statistical tests were performed on EEG and NIRS signals to find the most informative parameters. Fisher's linear discriminant analysis method was employed to classify awake and drowsy states. Time series analysis was used to predict drowsiness.	The mean accuracy of the combined EEG/NIRS increases 8.7 percent compared to EEG alone and 5.5 percent compared to NIRS alone.
Open Access Dataset for EEG+NIRS Single-Trial Classification				
2017	Hybrid NIRS-EEG	An open access dataset is provided in this study for hybrid brain–computer interfaces (BCIs) using electroencephalography (EEG) and near-infrared spectroscopy (NIRS).	Two BCI experiments (left versus right hand motor imagery; mental arithmetic versus resting state) were done. The dataset was validated using baseline signal analysis methods, with which classification performance was evaluated for each modality and a combination of both modalities.	1) MI- and MA-related activations were classifiable over motor areas and front-parietal areas, respectively. 2) The approach used led to rather poorer decoding accuracies, the results obtained from time segmented data can

				provide additional time-related information on the dataset. For a similar reason, any channel or subject selection based was not performed on signal quality or decoding accuracy in the analysis, except for the illustration of log(p)-based scalp plots.
Open Access Repository for Hybrid EEG-NIRS Data				
	Hybrid NIRS-EEG	In the present study, to meet the increasing demand on a hybrid brain imaging data, an open access data set of electroencephalography (EEG) and near-infrared spectroscopy (NIRS) simultaneously measured during various cognitive tasks is introduced. The datasets contain BCI data such as motor imagery (MI)-, and mental arithmetic (MA), and word generation (WG)-related brain signals, and cognitive task data such as n-back (NB)-, and discrimination/selection response (DSR)-related brain signals.	1) Down sampling EEG data. 2) Band-pass filter. 3) ICA- for EOG rejection. 4) Common spatial patterns. 5) Linear discriminant analysis.	75.9 % and 86.2 % of the participants show improved performance by the hybrid approach for MI and MA, respectively. The performance of 74.2 % of the participants are significantly improved by the hybrid approach than EE.
An EEG-NIRS Multimodal SoC for Accurate Anesthesia Depth Monitoring				
2018	Hybrid NIRS-EEG	In this paper, a multimodal head-patch system that simultaneously measures EEG and near Infrared spectroscopy (NIRS) on the frontal lobe is proposed for monitoring accurate anesthesia depth.	Logarithmic transimpedance amplifier (TIA) and closed loop controlled (CLC) NIRS current driver are proposed in the paper.	

A Comparison of EEG and NIRS Biomarkers for Assessment of Depression Risk				
2018	Hybrid NIRS-EEG	This study assesses the Frontal Alpha Asymmetry (FAA) obtained from EEG data at the resting-state and Laterality Index at Rest (LIR) given from NIRS data for detection of depression risk in the early stage. The Comfort Vector model (CVM) is another potential biomarker using the feature value of prefrontal alpha wave fluctuation.	Simultaneous NIRS and EEG recordings were performed during the resting-state for 5 minutes, and then FAA, LIR, emotional valence and arousal were obtained. Then, each participant performed the BDI test. Employing Pearson's correlation analysis, the correlations between the self-report inventories and the diagnostic markers were evaluated.	These correlations need further analysis with sample data of longer periods so that a regression model to combine the potential biomarkers can be developed.
Computational Pipeline for NIRS-EEG Joint Imaging of tDCS-Evoked Cerebral Responses—An Application in Ischemic Stroke				
2016	Hybrid NIRS-EEG	A software pipeline is presented in this paper incorporating freely available software tools that can be used to target vascular territories with tDCS and develop a NIRS-EEG probe for joint imaging of tDCS-evoked responses.	The software pipeline incorporates freely available SimNIBS for calculations of electric fields (and Current density) induced by tDCS. The software pipeline incorporates the headModel module of the open-source MoBILAB toolbox for computing EEG forward and inverse resolutions to identify EEG scalp topography that can record from tDCS-affected brain regions. The software pipeline incorporates also the probe design module of the freely available Atlas Viewer software to compute NIRS forward models for developing source and detector probe geometry to cover tDCS-affected brain regions. For demonstration, the software pipeline was applied on the Colin27 average brain. Based on their prior work, a cross-correlation analysis approach is presented to capture the coupling relation between regional cerebral hemoglobin oxygen saturation and the log-transformed mean-power time-series for EEG in case of ischemic stroke survivor.	
Multichannel Wearable fNIRS-EEG System for Long-Term Clinical Monitoring				
Study on Multi-parameter Evaluation Method of VDT Visual Fatigue Based on EEG and NIRS				
2017	Hybrid NIRS-EEG	The purpose of this paper is to build a system that can collect	1. attend-to-ignore ratios (AIR) of SSVEP amplitude before and after experiment.	The cerebral blood oxygen saturation would decrease because of visual fatigue.

		EEG, SSVEP, ERP and blood oxygen signals at the same time. A more comprehensive and objective assessment of visual fatigue can be obtained by analyzing these signals.	2. analyzed EEG data with eight octave wavelet decomposition. 3. Calculated energy of each frequency band. 4. Analyzed blood oxygen saturation levels.	Results are almost consistent with previous relevant researches.

Table-II

Year	Modality	Objective	Methodology	Results
Concealed face recognition analysis based on Recurrence Plots				
2011	EEG	Use of Recurrence Plots (RPs) in order to discriminate between guilty and innocent subjects, using their single-trial ERPs	EEG data recording during Guilty Knowledge Test (GKT) followed by recurrence plots and RQA parameters	Some RQA variables in guilty subjects are significantly higher than innocent ones. The results also showed that appearance of the P300 component can increase determinism and synchronization, in brains' signals
Understanding Coupling and Synchronization in EEG of Epileptic Discharge Using Recurrence Plots with Varying Threshold				
2012	EEG	Understanding the synchronicity of epileptic discharge using the property of recurrence of dynamical systems	Evaluation of the synchronization index from the recurrence distribution of phase space with variations in the recurrence dynamics by varying the threshold	he results of synchronization index indicate that the enhanced synchronicity is observed during seizure and decreases to near baseline level following seizure
EEG-based emotion recognition using Recurrence Plot analysis and K nearest neighbor classifier				
2013	EEG	The classification of EEG correlates on emotion using Recurrence Plot	Recurrence Plot analysis to extract thirteen non-linear features from EEG. Then compared with feature extraction method based on spectral power analysis. The K nearest neighbor is applied to classify extracted features into the emotional states	Performance rates of 58.05%, 64.56% and 67.42% for 3 classes of valence, arousal and liking
Adaptive filtering of EEG and epilepsy detection using Recurrence Quantification Analysis				

2014	EEG	Adaptive filtering of Electroencephalogram (EEG) signal and epileptic seizure detection using Recurrence Quantification Analysis (RQA)	Adaptive filtering of EEG signal followed by its recurrence plot formation and recurrence quantification analysis to detect epilepsy	sensitivity and specificity, 97.4% and 93.5% respectively
Detecting epileptic electroencephalogram by Recurrence Quantification Analysis				
2016	EEG	Quantitative analysis of epileptic patient's and healthy subject's EEG to detect epilepsy	Average Diagonal Length, a parameter from Recurrence Quantification Analysis (RQA), was calculated to analyze the difference between normal EEG and epileptic EEG in, quantitatively	Compared with the healthy control subjects, the epileptic EEG is more regular and more certain, meanwhile, it is Average Diagonal Length is longer
Recurrence plot structure of motor-related human EEG				
2019	EEG	RP structure of EEG segments recorded in somatosensory cortex are related with motor executions	RP reconstruction of EMG and EEG data recorded during motor task accomplishment	In averaged EEG signal background activity is mostly characterized by the diagonal lines, while motor task execution is associated with increase of recurrence points density and the emergence of vertical and horizontal lines
Time-frequency and recurrence quantification analysis detect limb movement execution from EEG data				
2019	EEG	Application of recurrence quantification analysis (RQA) in detection of motor-related electroencephalograms (EEG)	RQA to reveal transitions of mu-rhythm dynamics extracted from multichannel EEG recorded in motor cortex	The results show that the considering RQA measures of EEG in time-frequency domain one can effectively reveal dynamical features of motor-related brain activity
Characterization of EEG Resting-state Activity in Alzheimer's Disease by Means of Recurrence Plot Analyses				
2019	EEG	Characterize EEG resting-state activity in Alzheimer's disease (AD) patient's vs healthy subjects based on recurrence quantification analysis	TREND, a linear regression coefficient over the recurrence point density RRτ and provides information on the non-stationarity of a process	These results suggest that the dynamic properties of EEG resting-state activity differ between controls and AD patients
Classification of Epileptic Seizures using Recurrence Plots and Machine Learning Techniques				
2019	EEG	To explore reliable and faster binary classification algorithms to develop real time seizure detection system	EEG feature extraction based on the Recurrence Plots (RP), and Recurrence Quantification Analysis (RQA) and then their classification using Artificial Neural Network (ANN), Probabilistic Neural Network (PNN) and Support Vector Machine (SVM)	91.2 % highest binary class accuracy achieved with SVM

Two Approaches to Machine Learning Classification of Time Series Based on Recurrence Plots				
2020	EEG	Binary classification of epileptic seizure from EEG using two ML classification approaches for quantitative analysis and image classification	Perceptron (with 7 layers) for quantitative analysis of Recurrence plots CNN (with 131 layer) for image (Recurrence plot) classification	97% with perceptron 98% with CNN

REFERENCES

[1] K. D. Tanner, "Issues in neuroscience education: Making connections," *CBE Life Sciences Education*, 2006.

[2] M. J. Khan and K.-S. Hong, "Passive BCI based on drowsiness detection: an fNIRS study," *Biomed. Opt. Express*, 2015.

[3] M. A. Tanveer, M. J. Khan, M. J. Qureshi, N. Naseer, and K.-S. Hong, "Enhanced Drowsiness Detection Using Deep Learning: An fNIRS Study," *IEEE Access*, 2019.

[4] K. S. Hong and M. J. Khan, "Hybrid brain-computer interface techniques for improved classification accuracy and increased number of commands: A review," *Frontiers in Neurorobotics*. 2017.

[5] "Human Factors," *Intell. Veh.*, pp. 345–394, Jan. 2018.

[6] A. Byrne, "Mental workload as a key factor in clinical decision making," *Adv. Heal. Sci. Educ.*, 2013.

[7] S. Bioulac *et al.*, "Risk of motor vehicle accidents related to sleepiness at the wheel: A systematic review and meta-analysis," *Sleep*. 2017.

[8] M. Saadati, J. Nelson, and H. Ayaz, "Convolutional Neural Network for Hybrid fNIRS-EEG Mental Workload Classification," in *International Conference on Applied Human Factors and Ergonomics*, 2019, pp. 221–232.

[9] J. M. Noyes and D. P. J. Bruneau, "A self-analysis of the NASA-TLX workload measure," *Ergonomics*, 2007.

[10] S. Paulhus, D.L., Vazire, "The Self-Report Method," *Handb. Res. methods Personal. Psychol.*, 2005.

[11] B. Cain, "A Review of the Mental Workload Literature," *Def. Res. Dev. Toronto*, 2007.

[12] T. Q. Tran, R. L. Boring, D. D. Dudenhoeffer, B. P. Hallbert, M. D. Keller, and T. M. Anderson, "Advantages and disadvantages of physiological assessment for next generation control room design," in *IEEE Conference on Human Factors and Power Plants*, 2007.

[13] X. Chen, B. Zhao, Y. Wang, S. Xu, and X. Gao, "Control of a 7-DOF Robotic Arm System With an SSVEP-Based BCI," *Int. J. Neural Syst.*, vol. 28 8, p. 1850018, 2018.

[14] S.-I. Choi *et al.*, "On the feasibility of using an ear-eeg to develop an endogenous brain-computer interface," *Sensors*, vol. 18, no. 9, p. 2856, 2018.

[15] M. Ferrari and V. Quaresima, "A brief review on the history of human functional near-infrared spectroscopy (fNIRS) development and fields of application," *Neuroimage*, vol. 63, no. 2, pp. 921–935, 2012.

[16] J. León-Carrión and U. León-Dom\'\inguez, "Functional near-infrared spectroscopy (fNIRS): principles and neuroscientific applications," in *Neuroimaging-Methods*, IntechOpen, 2012.

[17] N. Naseer and K. S. Hong, "fNIRS-based brain-computer interfaces: A review," *Frontiers in Human Neuroscience*. 2015.

[18] M. J. Khan and K.-S. Hong, "hybrid eeg--fnirs-Based eight-command Decoding for Bci: application to Quadcopter control," *Front. Neurorobot.*, vol. 11, p. 6, 2017.

[19] S. Weyand, K. Takehara-Nishiuchi, and T. Chau, "Weaning Off Mental Tasks to Achieve Voluntary Self-Regulatory Control of a Near-Infrared Spectroscopy Brain-Computer Interface," *IEEE Trans. Neural Syst. Rehabil. Eng.*, 2015.

[20] S. Barbosa, G. Pires, and U. Nunes, “Toward a reliable gaze-independent hybrid BCI combining visual and natural auditory stimuli,” *J. Neurosci. Methods,* 2016.

[21] Y. Li, G. Zhou, D. Graham, and A. Holtzhauer, “Towards an EEG-based brain-computer interface for online robot control,” *Multimed. Tools Appl.,* 2016.

[22] C. Canning and M. Scheutz, “Functional Near-Infrared Spectroscopy in Human-Robot Interaction,” *J. Human-Robot Interact.,* 2013.

[23] M. Rehan and K. S. Hong, “Robust synchronization of delayed chaotic FitzHugh-Nagumo neurons under external electrical stimulation,” *Comput. Math. Methods Med.,* 2012.

[24] R. A. Khan, N. Naseer, N. K. Qureshi, F. M. Noori, H. Nazeer, and M. U. Khan, “FNIRS-based Neurorobotic Interface for gait rehabilitation,” *J. Neuroeng. Rehabil.,* 2018.

[25] R. Holtzer, J. R. Mahoney, M. Izzetoglu, C. Wang, S. England, and J. Verghese, “Online fronto-cortical control of simple and attention-demanding locomotion in humans,” *Neuroimage,* 2015.

[26] N. Naseer, M. J. Hong, and K. S. Hong, “Online binary decision decoding using functional near-infrared spectroscopy for the development of brain-computer interface,” *Exp. Brain Res.,* 2014.

[27] J. D. R. Millán *et al.*, “Combining brain-computer interfaces and assistive technologies: State-of-the-art and challenges,” *Frontiers in Neuroscience*. 2010.

[28] M. Krauledat, M. Schröder, B. Blankertz, and K. R. Müller, “Reducing calibration time for brain-computer interfaces: A clustering approach,” in *Advances in Neural Information Processing Systems*, 2007.

[29] X. Zhang, L. Yao, X. Wang, J. Monaghan, and D. Mcalpine, “A Survey on Deep Learning based Brain Computer Interface: Recent Advances and New Frontiers,” *arXiv Prepr. arXiv1905.04149*, 2019.

[30] S. Brigadoi *et al.*, “Motion artifacts in functional near-infrared spectroscopy: A comparison of motion correction techniques applied to real cognitive data,” *Neuroimage*, 2014.

[31] G. Bauernfeind, S. C. Wriessnegger, I. Daly, and G. R. Müller-Putz, “Separating heart and brain: On the reduction of physiological noise from multichannel functional near-infrared spectroscopy (fNIRS) signals,” *J. Neural Eng.*, 2014.

[32] M. Wronkiewicz, E. Larson, and A. K. C. Lee, “Leveraging anatomical information to improve transfer learning in brain-computer interfaces,” *J. Neural Eng.,* 2015.

[33] V. Jayaram, M. Alamgir, Y. Altun, B. Scholkopf, and M. Grosse-Wentrup, “Transfer Learning in Brain-Computer Interfaces,” *IEEE Comput. Intell. Mag.*, 2016.

[34] T. J. Huppert, S. G. Diamond, M. A. Franceschini, and D. A. Boas, “HomER: A review of time-series analysis methods for near-infrared spectroscopy of the brain,” *Appl. Opt.*, 2009.

[35] W. Tu and S. Sun, “A subject transfer framework for EEG classification,” *Neurocomputing,* 2012.

[36] S. Fazli, F. Popescu, M. Danóczy, B. Blankertz, K. R. Müller, and C. Grozea, “Subject-independent mental state classification in single trials,” *Neural Networks*, 2009.

[37] F. Lotte and C. Guan, “Learning from other subjects helps reducing brain-computer interface calibration time,” in *ICASSP, IEEE International Conference on Acoustics, Speech and Signal Processing - Proceedings*, 2010.

[38] "Handbook of research methods in personality psychology," *Choice Rev. Online*, 2007.

[39] R. Abiri, X. Zhao, G. Heise, Y. Jiang, and F. Abiri, "Brain computer interface for gesture control of a social robot: An offline study," in *Electrical Engineering (ICEE), 2017 Iranian Conference on*, 2017, pp. 113–117.

[40] U. Chaudhary, N. Birbaumer, and A. Ramos-Murguialday, "Brain--computer interfaces for communication and rehabilitation," *Nat. Rev. Neurol.*, vol. 12, no. 9, p. 513, 2016.

[41] A. Ortiz-Rosario and H. Adeli, "Brain-computer interface technologies: from signal to action," *Rev. Neurosci.*, vol. 24, no. 5, pp. 537–552, 2013.

[42] I. Volosyak, "SSVEP-based Bremen--BCI interface—boosting information transfer rates," *J. Neural Eng.*, vol. 8, no. 3, p. 36020, 2011.

[43] K.-S. Hong, M. J. Khan, and M. J. Hong, "Feature extraction and classification methods for hybrid fNIRS-EEG brain-computer interfaces," *Front. Hum. Neurosci.*, vol. 12, 2018.

[44] E. Erkan and M. Akbaba, "A study on performance increasing in SSVEP based BCI application," *Eng. Sci. Technol. an Int. J.*, vol. 21, no. 3, pp. 421–427, 2018.

[45] X. Gao, D. Xu, M. Cheng, and S. Gao, "A BCI-based environmental controller for the motion-disabled," *IEEE Trans. neural Syst. Rehabil. Eng.*, vol. 11, no. 2, pp. 137–140, 2003.

[46] M. Causse, Z. Chua, V. Peysakhovich, N. Del Campo, and N. Matton, "Mental workload and neural efficiency quantified in the prefrontal cortex using fNIRS," *Sci. Rep.*, 2017.

[47] P. H. S. Pelicioni, M. Tijsma, S. R. Lord, and J. Menant, "Prefrontal cortical activation measured by fNIRS during walking: effects of age, disease and secondary task," *PeerJ*, 2019.

[48] F. Al-Shargie, T. B. Tang, and M. Kiguchi, "Stress Assessment Based on Decision Fusion of EEG and fNIRS Signals," *IEEE Access*, 2017.

[49] N. Thanh Hai, N. Q. Cuong, T. Q. Dang Khoa, and V. Van Toi, "Temporal hemodynamic classification of two hands tapping using functional near-infrared spectroscopy," *Front. Hum. Neurosci.*, 2013.

[50] J. Xie *et al.*, "The role of visual noise in influencing mental load and fatigue in a steady-state motion visual evoked potential-based brain-computer Interface," *Sensors*, vol. 17, no. 8, p. 1873, 2017.

[51] Y.-J. Chen, S.-C. Chen, I. Zaeni, and C.-M. Wu, "Fuzzy tracking and control algorithm for an SSVEP-based BCI system," *Appl. Sci.*, vol. 6, no. 10, p. 270, 2016.

[52] S. Mendis, P. Puska, B. Norrving, World Health Organization., World Heart Federation., and World Stroke Organization., "WHO | Global atlas on cardiovascular disease prevention and control," *Who*, 2011.

[53] Centers for Disease Control and Prevention, "Underlying Cause of Death 1999-2010," *CDC WONDER Database*. 2020.

[54] B. Xiao, Y. Xu, X. Bi, J. Zhang, and X. Ma, "Heart sounds classification using a novel 1-D convolutional neural network with extremely low parameter consumption," *Neurocomputing*, 2020.

[55] Z. Jiang and S. Choi, "A cardiac sound characteristic waveform method for in-home heart disorder monitoring with electric stethoscope," *Expert Syst. Appl.*, 2006.

[56] L. Jin and J. Dong, "Classification of normal and abnormal ECG records using lead convolutional neural network and rule inference," *Sci. China Inf. Sci.*, 2017.

[57] P. Wang, J. Lu, B. Zhang, and Z. Tang, “A review on transfer learning for brain-computer interface classification,” in *2015 5th International Conference on Information Science and Technology (ICIST)*, 2015, pp. 315–322.

[58] S. J. Pan and Q. Yang, “A survey on transfer learning,” *IEEE Transactions on Knowledge and Data Engineering*. 2010.

[59] H. A. Abbass, J. Tang, R. Amin, M. Ellejmi, and S. Kirby, “Augmented cognition using real-time EEG-based adaptive strategies for air traffic control,” in *Proceedings of the Human Factors and Ergonomics Society*, 2014.

[60] S. W. Min *et al.*, “Erratum to Acetylation of tau inhibits its degradation and contributes to tauopathy,” *Neuron*. 2010.

[61] K. S. Hong and N. Naseer, “Reduction of delay in detecting initial dips from functional near-infrared spectroscopy signals using vector-based phase analysis,” *Int. J. Neural Syst.*, 2016.

[62] F. Al-Shargie, T. B. Tang, and M. Kiguchi, “Assessment of mental stress effects on prefrontal cortical activities using canonical correlation analysis: an fNIRS-EEG study,” *Biomed. Opt. Express*, vol. 8, no. 5, p. 2583, 2017.

[63] A. Curtin and H. Ayaz, “The Age of Neuroergonomics: Towards Ubiquitous and Continuous Measurement of Brain Function with fNIRS,” *Jpn. Psychol. Res.*, 2018.

[64] W. Glannon, “Ethical issues with brain-computer interfaces,” *Front. Syst. Neurosci.*, 2014.

[65] M. J. Khan, M. J. Hong, and K.-S. Hong, “Decoding of four movement directions using hybrid NIRS-EEG brain-computer interface,” *Front. Hum. Neurosci.*, vol. 8, p. 244, 2014.

[66] B. Z. Allison, C. Brunner, V. Kaiser, G. R. Müller-Putz, C. Neuper, and G. Pfurtscheller, “Toward a hybrid brain-computer interface based on imagined movement and visual attention,” *J. Neural Eng.*, 2010.

[67] G. Müller-Putz *et al.*, “Towards noninvasive hybrid brain-computer interfaces: Framework, practice, clinical application, and beyond,” *Proc. IEEE*, 2015.

[68] H. O. Keles, R. L. Barbour, and A. Omurtag, “Hemodynamic correlates of spontaneous neural activity measured by human whole-head resting state EEG + fNIRS,” *Neuroimage*, 2016.

[69] L. F. Nicolas-Alonso and J. Gomez-Gil, “Brain computer interfaces, a review,” *Sensors*. 2012.

[70] M. A. Franceschini, D. K. Joseph, T. J. Huppert, S. G. Diamond, and D. A. Boas, “Diffuse optical imaging of the whole head,” *J. Biomed. Opt.*, 2006.

[71] N. Naseer, N. K. Qureshi, F. M. Noori, and K. S. Hong, “Analysis of Different Classification Techniques for Two-Class Functional Near-Infrared Spectroscopy-Based Brain-Computer Interface,” *Comput. Intell. Neurosci.*, 2016.

[72] A. Zafar and K. S. Hong, “Neuronal Activation Detection Using Vector Phase Analysis with Dual Threshold Circles: A Functional Near-Infrared Spectroscopy Study,” *Int. J. Neural Syst.*, 2018.

[73] M. E. Spira and A. Hai, “Multi-electrode array technologies for neuroscience and cardiology,” *Nature Nanotechnology*. 2013.

[74] S. D. Power, A. Kushki, and T. Chau, “Intersession consistency of single-trial classification of the prefrontal

response to mental arithmetic and the no-control state by NIRS," *PLoS One*, 2012.

[75] U. Asgher, R. Ahmad, N. Naseer, Y. Ayaz, M. J. Khan, and M. K. Amjad, "Assessment and Classification of Mental Workload in the Prefrontal Cortex (PFC) using Fixed-Value Modified Beer-Lambert Law," *IEEE Access*, 2019.

[76] Y. Li *et al.*, "An EEG-based BCI system for 2-D cursor control by combining Mu/Beta rhythm and P300 potential," *IEEE Trans. Biomed. Eng.*, 2010.

[77] F.-M. Lu and Z. Yuan, "PET/SPECT molecular imaging in clinical neuroscience: recent advances in the investigation of CNS diseases.," *Quant. Imaging Med. Surg.*, 2015.

[78] N. Weiskopf *et al.*, "Principles of a brain-computer interface (BCI) based on real-time functional magnetic resonance imaging (fMRI)," *IEEE Trans. Biomed. Eng.*, 2004.

[79] J. D. Rieke *et al.*, "Development of a combined, sequential real-time fMRI and fNIRS neurofeedback system to enhance motor learning after stroke," *J. Neurosci. Methods*, 2020.

[80] S. B. Borgheai *et al.*, "Enhancing Communication for People in Late-Stage ALS Using an fNIRS-Based BCI System," *IEEE Trans. Neural Syst. Rehabil. Eng.*, 2020.

[81] J. B. F. Van Erp, F. Lotte, and M. Tangermann, "Brain-computer interfaces: Beyond medical applications," *Computer (Long. Beach. Calif).*, 2012.

[82] R. Rao and R. Scherer, "Brain-Computer Interfacing [In the Spotlight," *IEEE Signal Process. Mag.*, 2010.

[83] L. Bi, X.-A. Fan, and Y. Liu, "EEG-based brain-controlled mobile robots: a survey," *IEEE Trans. human-machine Syst.*, vol. 43, no. 2, pp. 161–176, 2013.

[84] A. A. Navarro *et al.*, "Context-awareness as an enhancement of brain-computer interfaces," in *Lecture Notes in Computer Science (including subseries Lecture Notes in Artificial Intelligence and Lecture Notes in Bioinformatics)*, 2011.

[85] K. S. Hong, M. J. Khan, and M. J. Hong, "Feature Extraction and Classification Methods for Hybrid fNIRS-EEG Brain-Computer Interfaces," *Frontiers in Human Neuroscience*. 2018.

[86] U. Asgher *et al.*, "Enhanced Accuracy for Multiclass Mental Workload Detection Using Long Short-Term Memory for Brain–Computer Interface," *Front. Neurosci.*, 2020.

[87] I. Chivers and J. Sleightholme, "An introduction to Algorithms and the Big O Notation," in *Introduction to Programming with Fortran*, Springer, 2015, pp. 359–364.

[88] A. Tharwat, T. Gaber, A. Ibrahim, and A. E. Hassanien, "Linear discriminant analysis: A detailed tutorial," *AI Commun.*, 2017.

[89] M. Sharir and M. H. Overmars, "A simple output-sensitive algorithm for hidden surface removal," *ACM Trans. Graph.*, 1992.

[90] M. Taghavi and M. Shoaran, "Hardware complexity analysis of deep neural networks and decision tree ensembles for real-time neural data classification," in *2019 9th International IEEE/EMBS Conference on Neural Engineering (NER)*, 2019, pp. 407–410.

[91] R. Pascanu, C. Gulcehre, K. Cho, and Y. Bengio, "How to construct deep recurrent neural networks," in *2nd International Conference on Learning Representations, ICLR 2014 - Conference Track Proceedings*, 2014.

[92] S. Zhang *et al.*, “Architectural complexity measures of recurrent neural networks,” in *Advances in Neural Information Processing Systems*, 2016.

[93] U. Asgher, K. Khalil, Y. Ayaz, R. Ahmad, and M. J. Khan, “Classification of Mental Workload (MWL) using Support Vector Machines (SVM) and Convolutional Neural Networks (CNN),” in *2020 3rd International Conference on Computing, Mathematics and Engineering Technologies: Idea to Innovation for Building the Knowledge Economy, iCoMET 2020*, 2020.

[94] Y. Blokland *et al.*, “Combined EEG-fNIRS decoding of motor attempt and imagery for brain switch control: an offline study in patients with tetraplegia,” *IEEE Trans. neural Syst. Rehabil. Eng.*, vol. 22, no. 2, pp. 222–229, 2014.

[95] C.-C. Lo, T.-Y. Chien, Y.-C. Chen, S.-H. Tsai, W.-C. Fang, and B.-S. Lin, “A wearable channel selection-based brain-computer interface for motor imagery detection,” *Sensors*, vol. 16, no. 2, p. 213, 2016.

[96] K.-S. Hong and H. Santosa, “Decoding four different sound-categories in the auditory cortex using functional near-infrared spectroscopy,” *Hear. Res.*, vol. 333, pp. 157–166, 2016.

[97] Z. Wu, Y. Lai, Y. Xia, D. Wu, and D. Yao, “Stimulator selection in SSVEP-based BCI,” *Med. Eng. Phys.*, vol. 30, no. 8, pp. 1079–1088, 2008.

[98] A. Floriano, P. F Diez, and T. Freire Bastos-Filho, “Evaluating the influence of chromatic and luminance stimuli on SSVEPs from behind-the-ears and occipital areas,” *Sensors*, vol. 18, no. 2, p. 615, 2018.

[99] P. F. Diez *et al.*, “Commanding a robotic wheelchair with a high-frequency steady-state visual evoked potential based brain--computer interface,” *Med. Eng. Phys.*, vol. 35, no. 8, pp. 1155–1164, 2013.

[100] J. Li, J. Liang, Q. Zhao, J. Li, K. Hong, and L. Zhang, “Design of assistive wheelchair system directly steered by human thoughts,” *Int. J. Neural Syst.*, vol. 23, no. 03, p. 1350013, 2013.

[101] C. S. Herrmann, “Human EEG responses to 1--100 Hz flicker: resonance phenomena in visual cortex and their potential correlation to cognitive phenomena,” *Exp. brain Res.*, vol. 137, no. 3–4, pp. 346–353, 2001.

[102] A. Kuś Rafałand Duszyk *et al.*, “On the quantification of SSVEP frequency responses in human EEG in realistic BCI conditions,” *PLoS One*, vol. 8, no. 10, p. e77536, 2013.

[103] G. R. Müller-Putz, R. Scherer, C. Brauneis, and G. Pfurtscheller, “Steady-state visual evoked potential (SSVEP)-based communication: impact of harmonic frequency components,” *J. Neural Eng.*, vol. 2, no. 4, p. 123, 2005.

[104] R. Abiri, S. Borhani, E. W. Sellers, Y. Jiang, and X. Zhao, “A comprehensive review of EEG-based brain-computer interface paradigms,” *J. Neural Eng.*, 2018.

[105] S. W. Brose *et al.*, “The role of assistive robotics in the lives of persons with disability,” *Am. J. Phys. Med. Rehabil.*, vol. 89, no. 6, pp. 509–521, 2010.

[106] Á. Fernández-Rodr\'\iguez, F. Velasco-Álvarez, and R. Ron-Angevin, “Review of real brain-controlled wheelchairs,” *J. Neural Eng.*, vol. 13, no. 6, p. 61001, 2016.

[107] A. Rezeika, M. Benda, P. Stawicki, F. Gembler, A. Saboor, and I. Volosyak, “Brain--computer interface spellers: A review,” *Brain Sci.*, vol. 8, no. 4, p. 57, 2018.

[108] D. Zhang, B. Huang, W. Wu, and S. Li, “An idle-state detection algorithm for SSVEP-based brain--

computer interfaces using a maximum evoked response spatial filter," *Int. J. Neural Syst.*, vol. 25, no. 07, p. 1550030, 2015.

[109] E. Galy, M. Cariou, and C. Mélan, "What is the relationship between mental workload factors and cognitive load types?," *Int. J. Psychophysiol.*, 2012.

[110] R. Hosseini, B. Walsh, F. Tian, and S. Wang, "An fNIRS-Based Feature Learning and Classification Framework to Distinguish Hemodynamic Patterns in Children Who Stutter," *IEEE Trans. Neural Syst. Rehabil. Eng.*, 2018.

[111] C. Herff, D. Heger, F. Putze, J. Hennrich, O. Fortmann, and T. Schultz, "Classification of mental tasks in the prefrontal cortex using fNIRS," in *Proceedings of the Annual International Conference of the IEEE Engineering in Medicine and Biology Society, EMBS*, 2013.

[112] L. C. Schudlo and T. Chau, "Dynamic topographical pattern classification of multichannel prefrontal NIRS signals: II. Online differentiation of mental arithmetic and rest," *J. Neural Eng.*, 2014.

[113] M. V. Kosti, K. Georgiadis, D. A. Adamos, N. Laskaris, D. Spinellis, and L. Angelis, "Towards an affordable brain computer interface for the assessment of programmers' mental workload," *Int. J. Hum. Comput. Stud.*, 2018.

[114] D. J. McFarland, W. A. Sarnacki, and J. R. Wolpaw, "Brain-computer interface (BCI) operation: Optimizing information transfer rates," *Biol. Psychol.*, 2003.

[115] B. Obermaier, C. Neuper, C. Guger, and G. Pfurtscheller, "Information transfer rate in a five-classes brain-computer interface," *IEEE Trans. Neural Syst. Rehabil. Eng.*, 2001.

[116] N. Naseer and K. S. Hong, "Classification of functional near-infrared spectroscopy signals corresponding to the right- and left-wrist motor imagery for development of a brain-computer interface," *Neurosci. Lett.*, 2013.

Proposed Certificate for Plagiarism

It is certified that PhD/M.Phil/MS Thesis Titled **EEG-fNIRS Based Image Reconstructuin and Classification for BCI** by **Nabeeha Ehsan Mughal** has been examined by us. We undertake the follows:

a. Thesis has significant new work/knowledge as compared already published or are under consideration to be published elsewhere. No sentence, equation, diagram, table, paragraph or section has been copied verbatim from previous work unless it is placed under quotation marks and duly referenced.
b. The work presented is original and own work of the author (i.e. there is no plagiarism). No ideas, processes, results or words of others have been presented as Author own work.
c. There is no fabrication of data or results which have been compiled/analyzed.
d. There is no falsification by manipulating research materials, equipment or processes, or changing or omitting data or results such that the research is not accurately represented in the research record.
e. The thesis has been checked using TURNITIN (copy of originality report attached) and found within limits as per HEC plagiarism Policy and instructions issued from time to time.

Name & Signature of Supervisor

Dr. Muhammad Jawad Khan

Signature : _____.